NACA RM A51G10

NACA

RESEARCH MEMORANDUM

PRELIMINARY INVESTIGATION OF THE PRESSURE FLUCTUATIONS IN THE WAKES OF TWO-DIMENSIONAL WINGS AT LOW ANGLES OF ATTACK

By Robert M. Sorenson, John A. Wyss,
and James C. Kyle

Ames Aeronautical Laboratory
Moffett Field, Calif.

NATIONAL ADVISORY COMMITTEE
FOR AERONAUTICS

WASHINGTON
October 30, 1951

NATIONAL ADVISORY COMMITTEE FOR AERONAUTICS

RESEARCH MEMORANDUM

PRELIMINARY INVESTIGATION OF THE PRESSURE FLUCTUATIONS IN THE WAKES OF TWO-DIMENSIONAL WINGS AT LOW ANGLES OF ATTACK

By Robert M. Sorenson, John A. Wyss,
and James C. Kyle

SUMMARY

The magnitudes of the pressure fluctuations were measured in the turbulent wakes of restrained two-dimensional airfoils at transonic speeds. The 4-foot-chord models had NACA 65_1-213 and 23013 wing sections. Detailed wake data for the model with the NACA 23013 section only are presented in this report through a range of Mach numbers from 0.6 to 0.8, a range of angles of attack from -2° to $+5^\circ$, and a range of Reynolds numbers from 9 to 11 million.

The measurements indicate that total-pressure fluctuations occurred only within the wake, that is, in the region of time-average total-pressure loss. Also, limited data indicate that, at least for the severest test condition, angle fluctuations were essentially within this wake. The maximum total-pressure fluctuations occurred in the portions of the wake where the gradients of the time-average total-pressure loss were maximum.

A method of defining wing buffet boundaries in terms of pressure fluctuations in the wake is discussed. Curves are presented showing the variation with Mach number of the wing lift coefficient at which horizontal tails at various locations would enter the irregular wake. Under such conditions tail buffeting could occur and thus a buffet boundary would be established. These curves are compared with the measured buffet boundary of an airplane having a similar wing section.

The frequencies of the pressure fluctuations in the wake appeared random unless periodic shock motion existed on the wing. With the appearance of shock oscillation, the oscillation frequency could sometimes be detected in the wake.

Buffeting frequencies from 16 to 20 cycles per second were found at 4° angle of attack on the airfoil with the NACA 23013 section. Frequencies on the airfoil with the NACA 65_1-213 section at 4° angle of attack varied from 20 to 25 cycles per second and from 45 to 55 cycles per second. For this model at 0° angle of attack, predominant buffeting frequencies were in the range of 41 to 44 cycles per second.

INTRODUCTION

Airplanes flying near the maximum lift coefficient at low subsonic speeds commonly encounter buffeting. This low-speed buffeting is attributed either to wing buffeting caused by areas of separated flow on the wing, or to tail buffeting caused by the tail entering the fluctuating wake emanating from regions of irregular flow.

Buffeting at transonic speeds is often encountered at lower lift coefficients and is usually attributed to shock-induced separation of the boundary layer on the wing. The frequent occurrence of tail buffeting under these conditions indicates the continuing need for quantitative evaluation of the flow fluctuations in the wakes of wings.

The flow separation precipitated by shock waves on the wing causes marked changes in the wake characteristics: the wake width sharply increases, and the irregularity of the flow in the wake becomes increasingly severe. (See reference 1.) In the rapidly oscillating flow over airfoils at supercritical speeds, both the angle of departure of the wake and the position of the shock wave may vary at high frequencies. (See reference 2.) Also, the frequency of shock-wave motion may couple with any wing motion such as aileron oscillation. (See reference 3.) Periodic pressure pulsations at shock-motion frequencies might, therefore, be expected in the wake. If the frequency of these pressure pulsations is near the natural frequencies of tail surfaces, there is a possibility of tail resonance. (See reference 4.)

Thus, some knowledge of the magnitude and frequency of total-pressure and stream-angle fluctuations in the wake is necessary in aircraft design concerned with minimizing tail buffeting. One of the few previous transonic investigations of the downwash fluctuations behind a three-dimensional, high-aspect-ratio wing was made by Ferri (reference 5).

The purpose of the present investigation was to obtain fundamental data on the vertical extent, magnitude, frequency, and other characteristics of the pressure fluctuations in the wakes of two-dimensional, restrained wings.

Total-pressure fluctuations in the wake were measured using electrical pressure cells. Similar pressure cells mounted flush with the wing surfaces were used to determine the amplitude and frequencies of wing-pressure changes for comparison with simultaneously measured pressure pulsations in the wake.

SYMBOLS

a	velocity of sound, feet per second
d	distance between point of minimum pressure and trailing edge of the airfoil, feet
f	frequency, cycles per second
f_a	aerodynamic frequency, cycles per second
h	average total-pressure loss in wake, pounds per square foot
Δh	double amplitude of total-pressure fluctuations in the wake, pounds per square foot
$\frac{h}{q}$	pressure-loss coefficient
$\frac{\Delta h}{q}$	pressure-fluctuation coefficient
M	free-stream Mach number
M_{cr}	critical Mach number
q	free-stream dynamic pressure, pounds per square foot
α	angle of attack, degrees

APPARATUS AND INSTRUMENTATION

Tunnel and Model

Two walls spaced 18.5 inches apart were installed in the Ames 16-foot high-speed wind tunnel to form a two-dimensional channel and the model was supported as shown in figure 1.

Measurements of the pressures along the walls of the two-dimensional channel were made with the model removed. Three horizontal rows of pressure orifices extending from the leading to the trailing edge were installed in each wall 9 inches apart, with the center row passing through the model location. The results shown in figure 2 are for the center row on one wall; the results for the other rows were essentially the same.

Without the model in place the total-pressure fluctuations between the walls, measured with the wake-survey instrument, were 1.0 percent or less of the free-stream dynamic pressure, while the stream-angle fluctuations were of the order of ±0.1.

The two 4-foot-chord models with NACA 23013 and 65_1-213 (a=0.5) sections had 18-1/8-inch spans. The spaces between the models and the mounting walls were sealed with sponge rubber. The models were of solid wood construction forward of the midchord with 1/8-inch, internally ribbed, aluminum plates from the midchord to the control hinge line. The chord of the flaps was 25 percent of the over-all chord, and the flaps were of wood-rib and stressed-skin construction. The flaps were restrained by means of a control-surface arm within the mounting walls. The flush-type, electrical pressure cells were located along the upper and lower surfaces at the middle of the span of the models.

Wake-Survey Instrument

A diagrammatic sketch of the experimental setup is shown in figure 3(a). The wake-survey instrument was attached to a horizontal sting which was supported by a vertical strut. The vertical position of the rake was adjusted as desired. An extension on the sting allowed the horizontal distance from the trailing edge of the model to the instrument to be changed from 70 percent to 20 percent of the airfoil chord.

The instrument to determine wake fluctuations by use of pressure cells 1/2 inch in diameter is shown in more detail in figure 3(b). The center cell was inset 1/8 inch while the upper and lower cells were flush with the surface. A typical record of the effect of air-stream turbulence at a Mach number of 0.8 with the tunnel empty is shown in figure 4(a). The turbulence in the wind tunnel was small in comparison with the magnitude of the fluctuations measured with the model in the tunnel. (See fig. 5.)

To determine whether the 1/8-inch-inset center pressure cell was insensitive to stream-angle fluctuations, the wake-survey instrument was oscillated at 5 and 10 cycles per second through an included pitch angle

of 8.5°. Typical records from such tests are shown in figure 4(b); they indicate the desired lack of sensitivity of the center pressure cell to changes in stream angle.

Since the dynamic pressure was constant during these tests, the electrical summation of the difference in pressure between the upper and lower cells shown in figure 4(b) indicates the effect of stream-angle variation. In figure 4(b), an upward movement of the traces indicates a decrease in pressure on the upper cell and an increase in pressure on the lower cell.

It must be recognized that with the wake survey instrument in the downwash of the model, and therefore at an angle to the local flow direction, a fluctuation of total pressure will cause an apparent angle change to be indicated by the upper and lower cells. Hence, the angle change indicated by the trace of the electrical summation of the two cells is affected by a fluctuation of total pressure, and a variation of stream angle, as well as other factors such as the phase relation between total-pressure and stream-angle fluctuations and the physical size of the wake survey instrument.

Even though the measured angle changes are not solely due to stream-angle fluctuations, the data do provide an indication of the vertical extent of stream-angle fluctuations in the wake. The measured angle variation indicated by the upper and lower pressure cells of the wake survey instrument is therefore defined as an effective stream-angle variation which can include factors other than stream-angle variation.

The pressure cells of the wake-survey instrument were capped and sealed to determine whether any pressure-cell response occurred due to the vibration of the wake-instrument support system by the fluctuating wake of the wing. That no such response occurred is illustrated in figure 5, which shows oscillograph traces from the center pressure cell in the capped and uncapped condition.

Static calibration of all pressure cells showed linear response to external pressure or vacuum, and the slope remained unchanged within the temperature and pressure range encountered during the tests.

Electrical Instrumentation

A block diagram of the electrical instrumentation used is shown in figure 6. The basic electronic apparatus described in reference 6 was used, although the carrier-current amplifier was modified to improve the frequency band pass.

A switching arrangement was provided so that visual as well as recorded data could be obtained. The visual data were read on a vacuum-tube voltmeter. Since the vacuum-tube voltmeter was calibrated to measure the root-mean-square value of the oscillating voltage, the average indicated values were multiplied by 1.414 to obtain the average peak-to-peak values. The value 1.414 was selected on the arbitrary assumption that nearly all the fluctuations were of a sinusoidal nature. The over-all frequency response showing the attenuation of the visual and recording systems is presented in figure 7. The amplitude response of the pressure cell was flat for the range of frequencies shown in figure 7.

Static calibrations of each pressure cell were made by changing the pressure in known increments inside the cell and reading the change in electrical output of the cells on a direct-current voltmeter.

TESTS

With the Mach number and angle of attack held constant and the wake-survey instrument 0.70-chord length behind the trailing edge of the airfoil, the wake-survey instrument was moved vertically through the wake, and data were taken from one-half chord length below to one chord length above the horizontal plane of the control-surface hinge line of the NACA 23013 airfoil. This procedure was repeated with the wake-survey instrument 0.2-chord length behind the trailing edge of the airfoil. The Mach number range was from 0.6 to 0.8 for angles of attack of -2°, 0°, $+2^\circ$, $+4^\circ$, and $+5^\circ$. The Mach numbers were corrected for constriction effects by the methods of reference 7. The Reynolds number varied from 9 to 11 million. For each test condition the average root-mean-square value of the total-pressure fluctuation in the wake was read on the vacuum-tube voltmeter. The average root-mean-square of the effective stream-angle fluctuations was obtained for an angle of attack of $+5^\circ$. Simultaneously, a photographic record was taken of the time-average total-pressure losses in the wake as indicated by the wake-survey rake and liquid-in-glass manometers. For some test conditions, in addition to the above data, oscillograph records were taken of pressure fluctuations in the wake and on the wing. The oscillograph records each covered a time interval of about 2 seconds, while the visual records of the vacuum-tube voltmeter were estimated averages for time intervals of about 20 seconds.

Oscillograph records were also taken to determine the frequencies of the pressure fluctuations on the surface and in the wake 70 percent of the chord behind the trailing edge of the NACA 65_1-213 airfoil.

RESULTS

Characteristics of the wake 0.70 chord behind the NACA 23013 airfoil are shown in figures 8 to 12, and in figures 13 to 17 they are shown for 20-percent chord behind the trailing edge of the wing. The time-average total-pressure loss, average pressure fluctuations, and, for angles of attack of 0° and 5°, the maximum pressure fluctuations are plotted in terms of vertical location. A large number of data points which define the total-pressure loss in the wake were omitted; the data points plotted in the figures are those taken as being representative of the time-average values. The average pressure fluctuation shown is the average double amplitude of the fluctuations obtained by multiplying the vacuum-tube voltmeter readings by 1.414, since the vacuum-tube voltmeter indicates root-mean-square values. The maximum pressure fluctuation shown is the average of the three largest peak-to-peak fluctuations on the oscillograph records.

The zeros of the ordinate scales in figures 8 to 17 represent the vertical location of the control-surface hinge line. Distances above and below the hinge line are given in percent of the airfoil chord and are positive for locations above the elevation of the hinge line. No attempt was made to correct measured values of fluctuations for attenuation of the oscillograph galvanometer elements because of the large range of frequencies in the data.

The effective stream-angle fluctuations, as indicated by the upper and lower pressure cells of the wake survey instrument, are compared with the time-average total-pressure loss in figure 18 to provide an indication of the vertical extent of stream-angle variation. The data presented in this figure were taken at 0.7 chord aft of the NACA 23013 airfoil.

The average effective stream-angle fluctuation is the average peak-to-peak values of the fluctuations obtained from vacuum-tube voltmeter readings multiplied by 1.414. The maximum effective stream-angle fluctuation is the average of the three largest peak-to-peak fluctuations on the oscillograph records.

DISCUSSION

Magnitude of Pressure Oscillation in the Wake

Examination of figures 8 through 17 shows that the total-pressure fluctuations did not extend outside the average wake and that they were characterized by peak values which always occurred on both sides of the

point of maximum total-pressure loss. These peaks occurred where the gradients of the total-pressure losses were maximum.

At 70-percent chord behind the trailing edge of the model for a 0° angle of attack, the average and maximum pressure fluctuations nearly corresponded and the region of pressure losses was small. With increase in angle of attack, the region of pressure losses and the intensity of pressure fluctuations sharply increased. Particularly, the maximum pressure fluctuations became of the same order of magnitude as the total-pressure loss, even though the average pressure fluctuations were considerably less. (See figs. 12(c) and 12(d).)

To indicate the Mach numbers at which the magnitude of the pressure fluctuation suddenly increased, a plot of the largest amplitudes of the average pressure fluctuations found in the wake 70-percent chord aft of the trailing edge is given as a function of Mach number in figure 19. It can be seen that the fluctuations held to a fairly constant amplitude until some Mach number was reached above which the rate of growth with further increase of Mach number became very rapid. Since the fluctuations originated on the wing, a wing buffet boundary was defined at those Mach numbers and lift coefficients where the initial increase in wake pressure fluctuations occurred. The Mach number for each angle of attack at which $\partial(\Delta h/q)/\partial M = 0.1$ was determined from figure 19. The corresponding lift coefficient was obtained from unpublished data for an NACA 23013 airfoil investigated in the Ames 1- by 3-1/2-foot wind tunnel. These data were plotted in figure 20 as the wing buffet boundary.

In addition to this boundary, other curves have been plotted in figure 20 which have been determined in an entirely different manner. Horizontal tails at arbitrary vertical locations were assumed to be 70 percent of the wing chord behind the trailing edge of the NACA 23013 airfoil. The Mach numbers and lift coefficients, at which tails in these assumed locations would be just entering the fluctuating wakes, were determined from figures 8 to 12. Under these conditions, tail buffeting could occur and therefore they are presented as buffet boundaries (fig. 20) for the various assumed tail locations.

The buffet boundary for a horizontal tail 18 percent of the wing chord above the wing-chord plane and the wing buffet boundary from figure 20 were corrected to an aspect ratio of 5.17, assuming elliptic wing loading and using the formulas developed in reference 8, page 145. These buffet boundaries are compared in figure 21 with a flight-determined buffet boundary of the Grumman F8F airplane. (See reference 9.) This airplane was selected for the comparison because its wing section was similar to that of the wind-tunnel model. The F8F airplane has an aspect ratio of 5.17 with an NACA 23018 root section and an NACA 23009 tip section. At the quarter-semispan wing location, the wing thickness

is about 16 percent. In the vertical plane passing through this section, the tail-surface orientation is 0.23-chord length above the wing-chord line extended, and 1.03-chord length behind the trailing edge of the wing. The similar trends of the buffet boundaries in figure 21 provide some indication of correlation even though the wing thickness and the assumed and actual tail locations are not exactly the same. Because of these differences, and since the airplane is subject to other three-dimensional effects, such as the interference caused by the wing-fuselage juncture, a more specific comparison of the curves cannot be made.

Effective Stream-Angle Fluctuations in the Wake

The effective stream-angle fluctuations were measured for an angle of attack of 5° for Mach numbers from 0.6 to 0.75 at the test station 0.7 chord behind the trailing edge. Typical of these results are the data shown in figure 18 for 0.75 Mach number. The severest fluctuations found in the investigation occurred for these conditions. Figure 18 shows that for these conditions the regions of angle fluctuation and of total-pressure loss nearly corresponded. It can be presumed that this conclusion would hold for lower angles of attack.

The total-pressure-fluctuation and angle-fluctuation data seem to be at variance with previous results since in references 5 and 10 fluctuations were reported to extend beyond the wake boundaries. Wake data presented in reference 5 were obtained 3.1 root chords behind the leading edge of a three-dimensional wing, while in the present investigation wake data were obtained 1.7 root chords behind the leading edge of a two-dimensional airfoil. These differences may account for the apparent discrepancies between the results. Although wake data behind a two-dimensional airfoil are reported in reference 10, comparison of the results with those of the present investigation is not possible because the instrumentation used by Duncan was insensitive to fluctuations for angles of attack less than 6° while the maximum angle of attack of the present investigation was 5°.

The data for total-pressure fluctuations shown in figure 12(d) were obtained under the same conditions as the data shown in figure 18. A comparison of these figures indicates that the regions of total-pressure fluctuations, effective angle fluctuations, and total-pressure loss were essentially the same. Since the measurements of effective or local angle fluctuation were influenced by the total-pressure fluctuations, the interrelation or possible mechanism that would explain the relation between the two variables of total pressure and angle variations has not been defined. Nevertheless, the regions of maximum fluctuations in the wake are clearly established.

Frequencies of Pressure Oscillation on the Wing and in the Wake

A study of oscillograph records for both models at 0° and 4° angle of attack showed that, unless a periodic shock motion existed on the wing as indicated by wing pressure fluctuations, no prevailing frequency could be determined from wake data. Rather, the pressure fluctuations were complex with random high frequencies. The oscillograph trace shown in figure 5 is typical.

However, with the appearance of a shock oscillation, its frequency could sometimes be detected in the wake. The apparent coupling between shock motion and the pressure pulsations in the wake is illustrated in figures 22(a) and 22(b) for the NACA 23013 and 65_1-213 airfoils, respectively.

The passage of the shock wave across the pressure cells at 25 and 35 percent of the chord (fig. 22(a)) results in the typical traces for these cells indicative of the large pressure change across the shock. (See reference 6, p.7.) It may be further noted that the pressure fluctuations along the airfoil surface are all at the frequency of shock motion although there is a readily apparent change in phase or time lag between any two chord locations. For example, the pressure fluctuations ahead of and behind the shock wave shown by the traces from pressure cells at 15 and 50 percent of the chord have an apparent phase difference of almost 180°. The frequency of shock motion is detectable in the trace from the center cell of the wake-survey instrument even though other frequencies of wake pressure fluctuations are present. In figure 22(b) the frequency of shock motion can be determined from the pressure fluctuations along the upper surface of the airfoil from 55 percent to 70 percent of the chord. The frequency of wake pressure fluctuation corresponding to shock motion is more readily apparent in the right-hand portion of the figure.

The frequency of shock motion on both models appeared intermittent, any one frequency sometimes persisting for as long as a second and at other times for only 2 or 3 cycles. Since shock oscillation did not always occur during the time interval during which oscillograph data were recorded, it was not possible to determine the vertical extent of detectably periodic pressure fluctuations in the wake.

For the NACA 23013 airfoil, periodic shock motion was detected only for an angle of attack of 4°. At 0.7 Mach number the shock oscillated at 16 cycles per second, and at 0.725 Mach number the frequency varied from 17 to 20 cycles per second. At the higher test Mach numbers, the shock motion was irregular with no determinable periodicity.

For the NACA 65_1-213 airfoil at 0° angle of attack periodic shock motions were indicated only at Mach numbers of 0.725 and 0.75, the frequencies of the motions being from 41 to 44 cycles per second. At the other test Mach numbers no prevailing frequencies were detected; rather, the pressure fluctuations were random. At 4° angle of attack two ranges of frequency of the shock-wave motion occurred as the Mach number was changed from 0.70 to 0.775. First, at Mach numbers from 0.70 to 0.725, frequencies of from 20 to 25 cycles per second were easily discerned as the shock motion consistently occurred at a uniform frequency and persisted for as long as a second. Second, at a Mach number of 0.775 the frequencies were from 45 to 55 cycles per second. However, at 0.75 Mach number the frequency was not so easily determined inasmuch as wing-surface pressure fluctuations were irregular. Nevertheless, for intervals of 2 to 3 cycles the frequency was fairly constant, the values ranging from 20 to 55 cycles per second, thus comprising both the above frequency ranges.

The distinct differences in frequencies between the forward-cambered, conventional NACA 23013 airfoil (16 to 20 cycles per second) and the low-drag NACA 65_1-213 airfoil (20 to 55 cycles per second) can be related to the general differences in pressure distributions of these two types of airfoils.

The chordwise pressure distribution at various Mach numbers for the NACA 23015 and NACA 65_1-215 sections is shown in figures 5(f) and 2(f), respectively, in reference 11. Although the airfoils of the present test were 13 percent thick, it is believed that qualitatively the pressure distributions are similar to those reported in reference 11. The conventional airfoil, at 4° angle of attack, has a well-defined minimum-pressure point ahead of the quarter-chord station for a Mach number range from below to well above the critical. On the other hand, the minimum-pressure point of the low-drag airfoil at 4° angle of attack is near the leading edge at the critical Mach number but rapidly approaches midchord as the Mach number increases.

A semiempirical equation for the aerodynamic or buffeting frequency, based on the time interval for a pressure impulse at the trailing edge to propagate forward to the shock position, is presented in reference 3. The equation takes the form:

$$f_a = \frac{a(1-M_{cr})}{4d}$$

The frequencies were calculated by using the distance to the point of minimum pressure and the critical Mach number of the section as recommended in the above report (reference 3, p. 15). For the NACA 23013 airfoil at 4° angle of attack, the computed frequency was 35.9 cycles per second as compared with 17 to 20 cycles per second from the test

data. For the NACA 65_1-213 airfoil at 4° angle of attack the comparison is 32 cycles per second from the formula with experimental frequencies of 20 to 55 cycles per second. At 0° angle of attack, the computed frequency was 42.5 cycles per second as compared with 41 to 44 cycles per second found in the test records.

While the computed and experimental frequencies do not agree for the conventional airfoil, it appears that the semiempirical equation can be used as a first approximation of the primary pressure fluctuations in the wake of the NACA 65_1-213 airfoil.

CONCLUDING REMARKS

An experimental investigation has been conducted to determine the magnitude and other characteristics of the pressure fluctuations in the turbulent wakes of two-dimensional airfoils.

The measurements indicate that total-pressure fluctuations occurred only within the wake, that is, in the region of time-average total-pressure loss. Also, limited data indicate that, at least for the severest test condition, angle fluctuations were essentially within this wake. The maximum pressure fluctuations occurred on both sides of the peak pressure loss in that portion of the wake where the pressure-loss gradients were maximum.

The frequencies of the pressure fluctuations in the wake appeared random unless periodic shock motion existed on the wing. With the appearance of shock oscillation, the same frequency could sometimes be detected in the wake. A semiempirical equation for the aerodynamic frequency does provide an estimate of the frequency of the primary periodic pressure fluctuations in the wake of the NACA 65_1-213 airfoil.

Ames Aeronautical Laboratory,
National Advisory Committee for Aeronautics,
Moffett Field, Calif.

REFERENCES

1. Stack, John: Compressible Flows in Aeronautics. Jour. Aero. Sci., vol. 12, no. 2, April, 1945, pp. 127-148.

2. Daley, Bernard N., and Humphreys, Milton D.: Effects of Compressibility on the Flow Past Thick Airfoil Sections. NACA TN 1657, 1948. (Formerly NACA RM L6J17a.)

3. Erickson, Albert L., and Stephenson, Jack D.: A Suggested Method of Analyzing for Transonic Flutter of Control Surfaces Based on Available Experimental Evidence. NACA RM A7F30, 1947.

4. Abdrashitov, G.: Tail Buffeting. NACA TM 1041, 1943.

5. Ferri, Antonio: Preliminary Investigation of Downwash Fluctuations of a High-Aspect-Ratio Wing in the Langley 8-Foot High-Speed Tunnel. NACA RM L6H28b, 1946.

6. Erickson, Albert L., and Robinson, Robert C.: Some Preliminary Results in the Determination of Aerodynamic Derivatives of Control Surfaces in the Transonic Speed Range by Means of a Flush-Type Electrical Pressure Cell. NACA RM A8H03, 1948.

7. Allen, H. Julian, and Vincenti, Walter G.: Wall Interference in a Two-Dimensional-Flow Wind Tunnel With Consideration of the Effect of Compressibility. NACA Rep. 782, 1944.

8. Glauert, H.: The Elements of Aerofoil and Airscrew Theory. Cambridge, Eng., The University Press, 1943, p. 145.

9. Gadeberg, Burnett L., and Ziff, Howard L.: Flight-Determined Buffet Boundaries of Ten Airplanes and Comparisons with Five Buffeting Criteria. NACA RM A50I27, 1951.

10. Duncan, W. J., Ellis, D. L., and Scruton, C.: First Report on the General Investigation of Tail Buffeting. R. & M. No. 1457, British A.R.C., 1932.

11. Graham, Donald J., Nitzberg, Gerald E., and Olson, Robert N.: A Systematic Investigation of Pressure Distributions at High Speeds Over Five Representative NACA Low-Drag and Conventional Airfoil Sections. NACA Rep. 832, 1945.

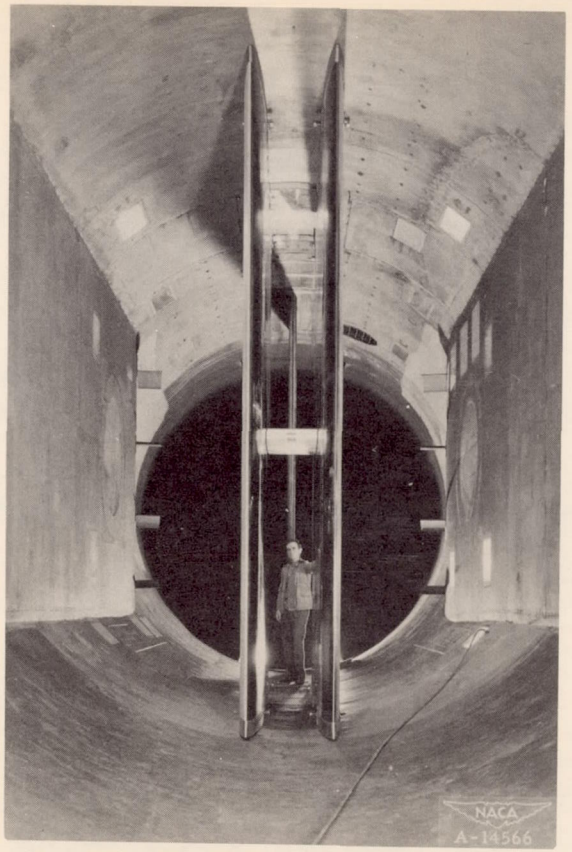

(a) Front view.

(b) Rear view.

Figure 1.–Views of test section with two-dimensional walls showing model and wake survey instrument support.

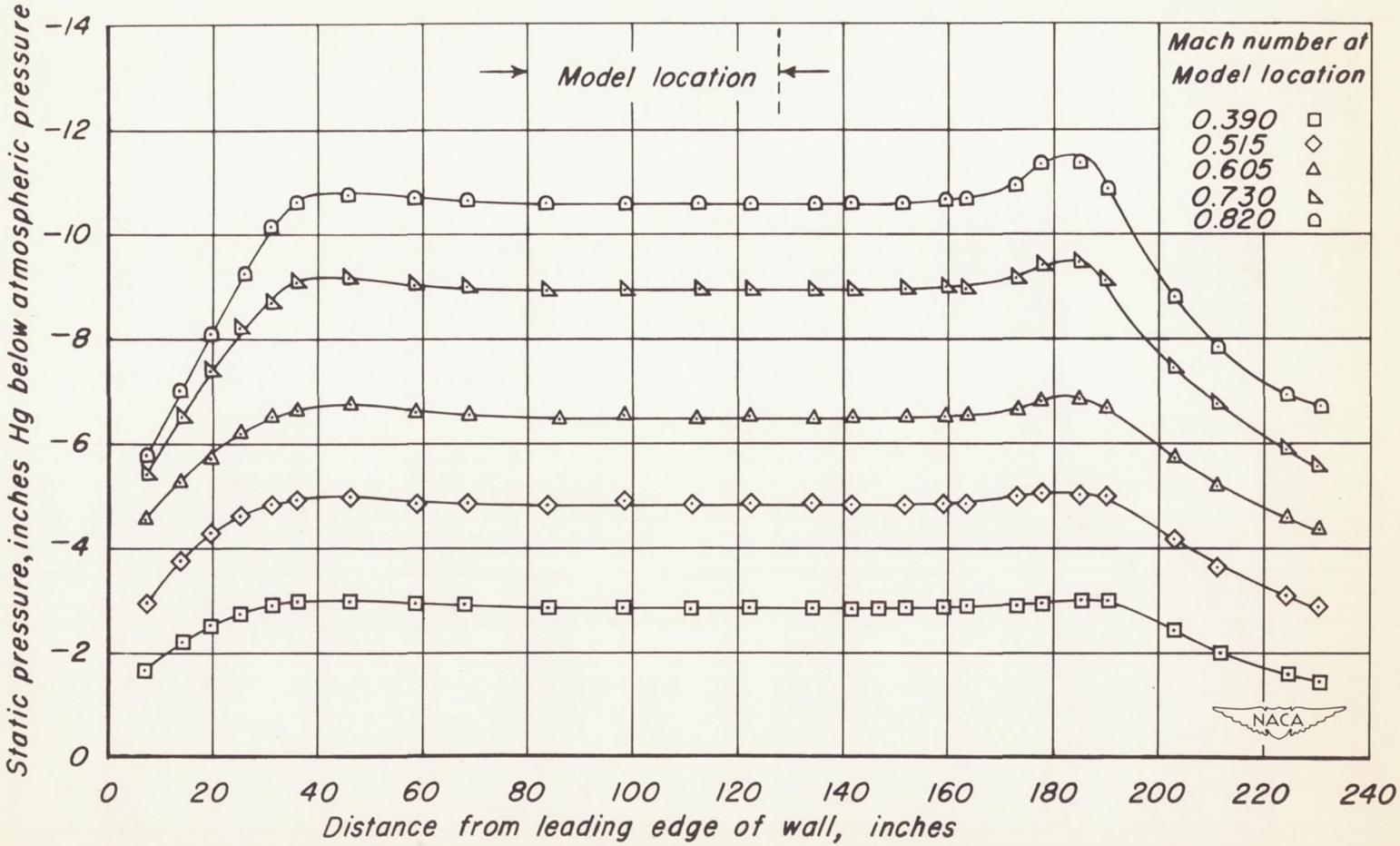

Figure 2.-Pressure distribution along two-dimensional test-section wall.

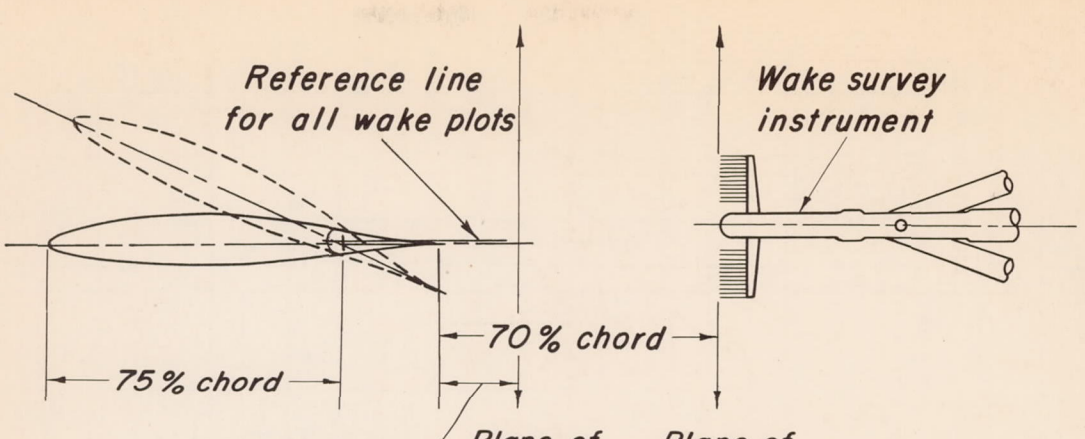

(a) Diagrammatic sketch of test setup.

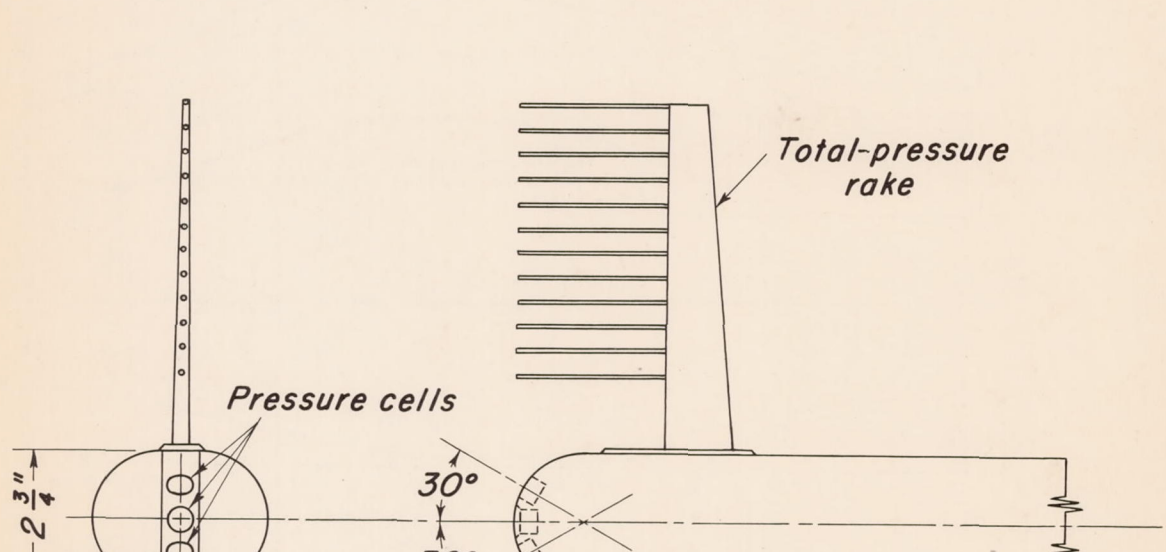

(b) Detail of wake survey instrument.

Figure 3.—Sketch of test setup and detail of wake instrument.

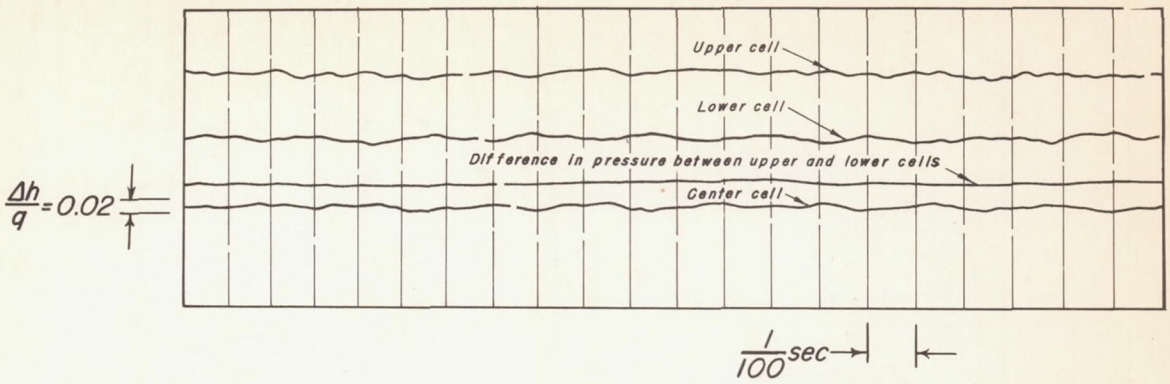

(a) Typical record indicating degree of tunnel turbulence.

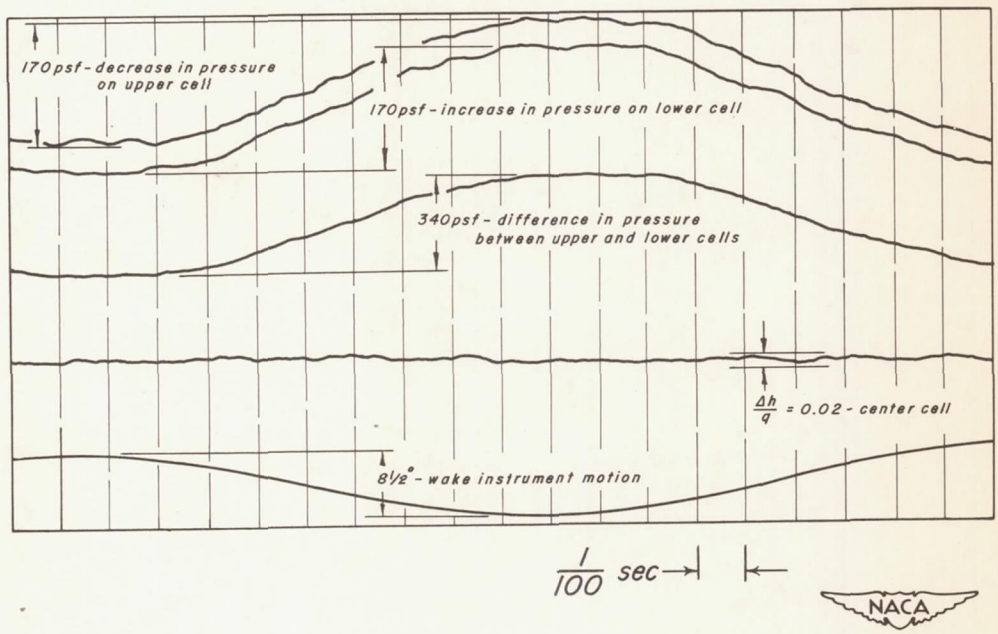

(b) Record illustrating the insensitivity of the center pressure cell to stream-angle effects.

Figure 4.- Records of pressure cells with wake intrument stationary and oscillating in pitch through an angle of $8\frac{1}{2}°$ at 5 cycles per second with the tunnel empty. M, 0.8.

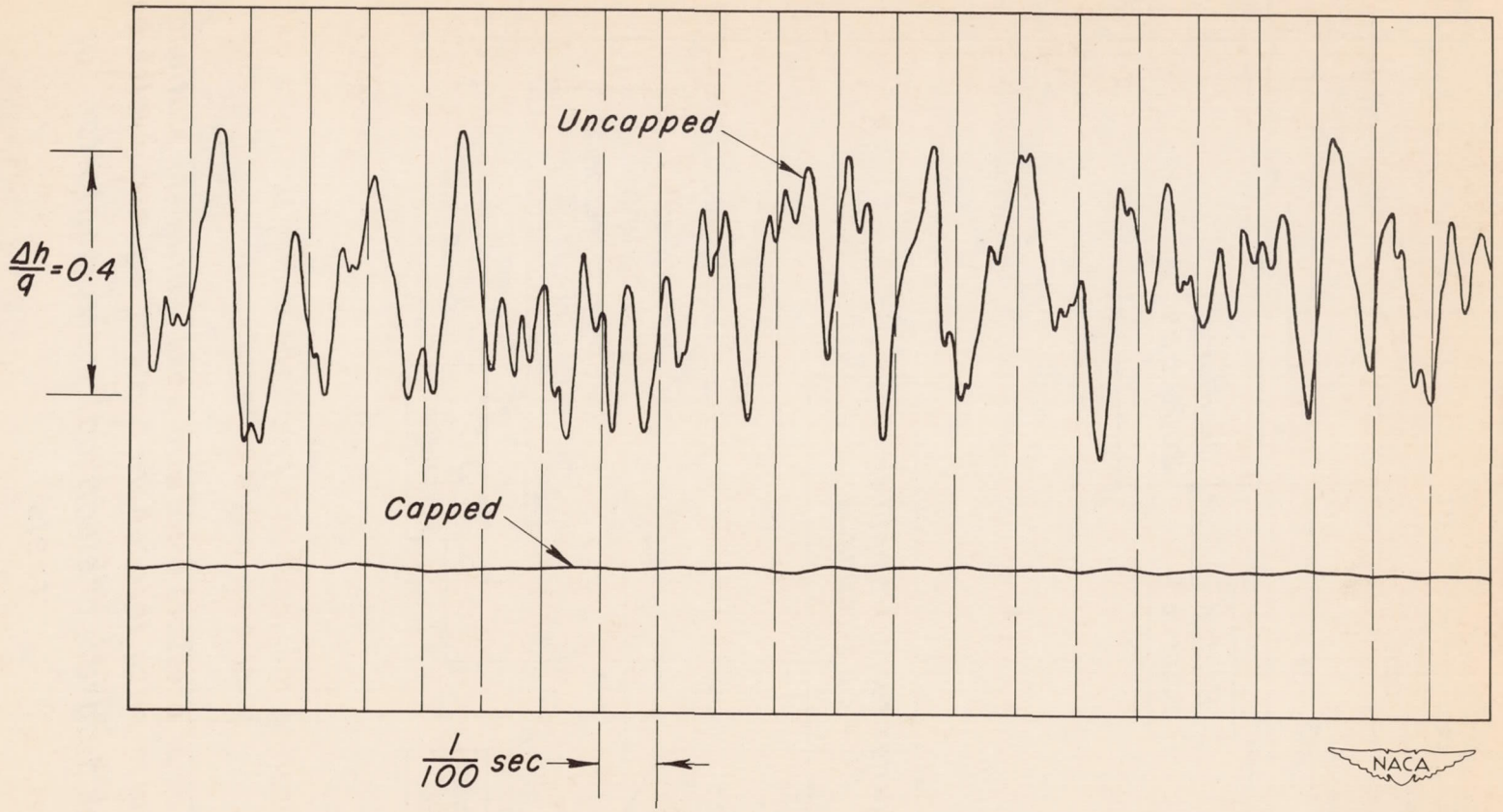

Figure 5.– Record from the center pressure cell, capped and uncapped, with the wake survey instrument at the zero position 70-percent-chord behind the trailing edge of the NACA 23013 airfoil, M, 0.775, α, +4°.

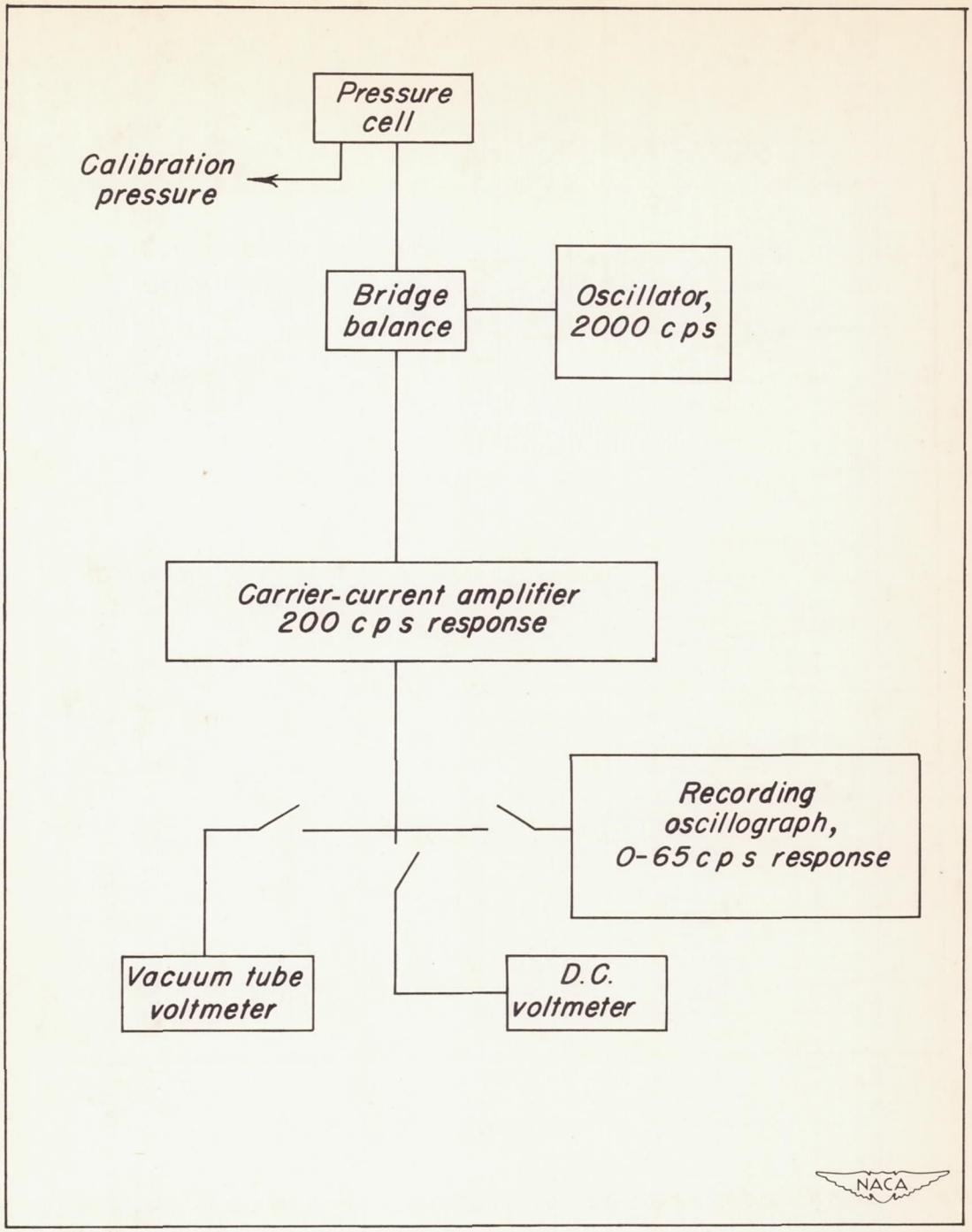

Figure 6.–Block diagram of electrical instrumentation for tests.

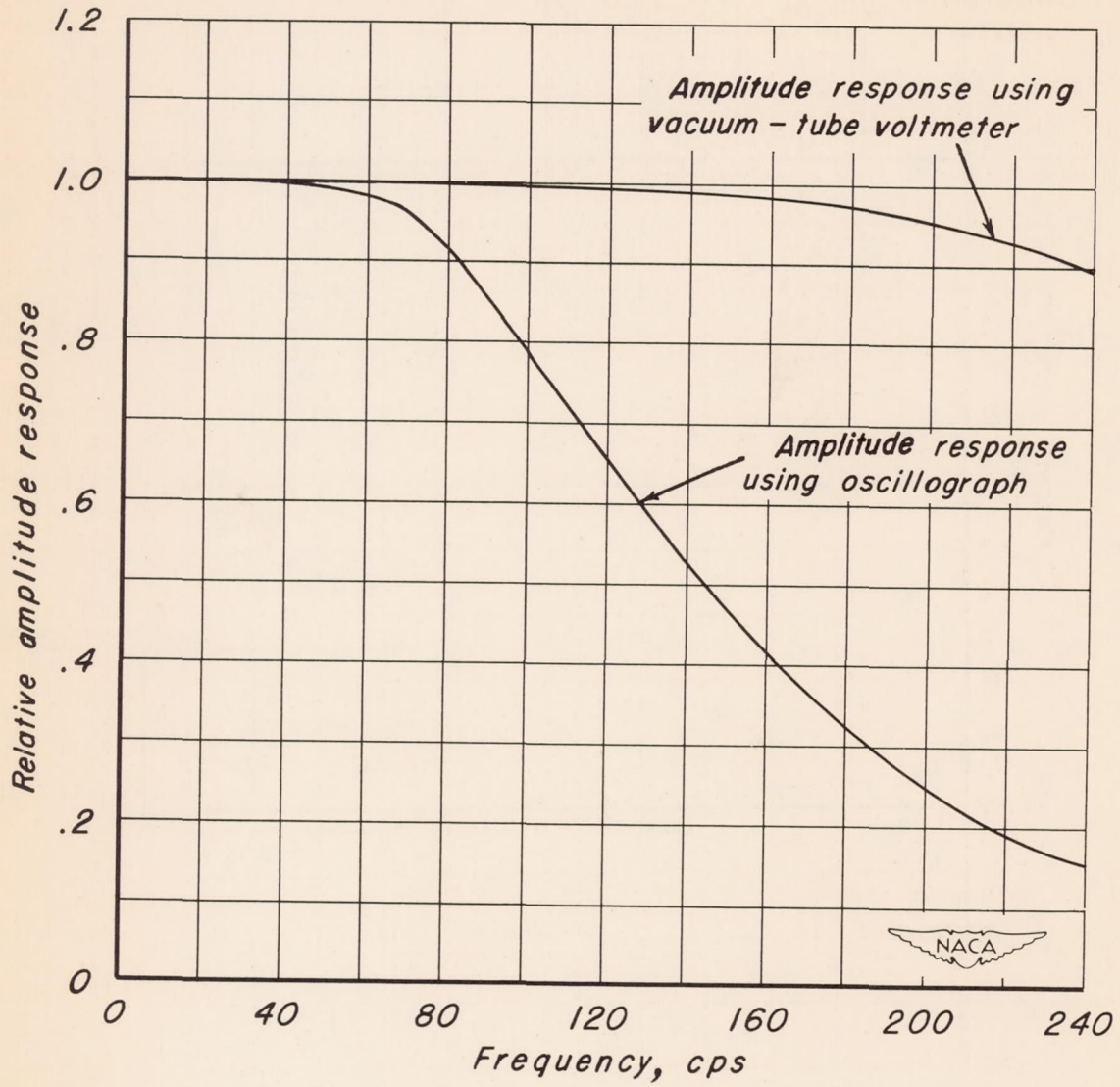

Figure 7.– Amplitude response of indicating and recording equipment.

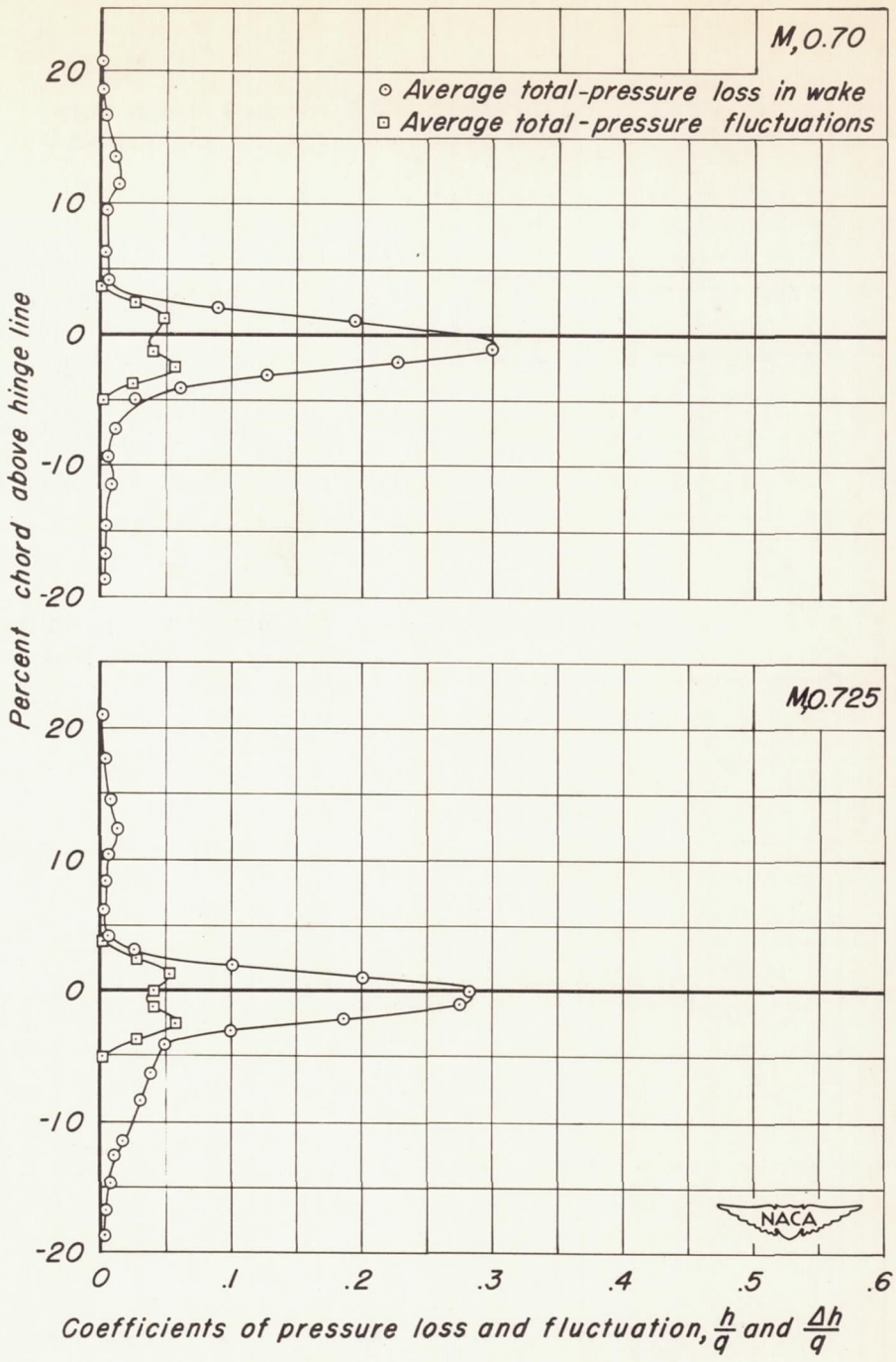

(a) M, 0.70 and 0.725

Figure 8.– Wake characteristics at 70-percent-chord aft of the NACA 23013 airfoil. α, -2°

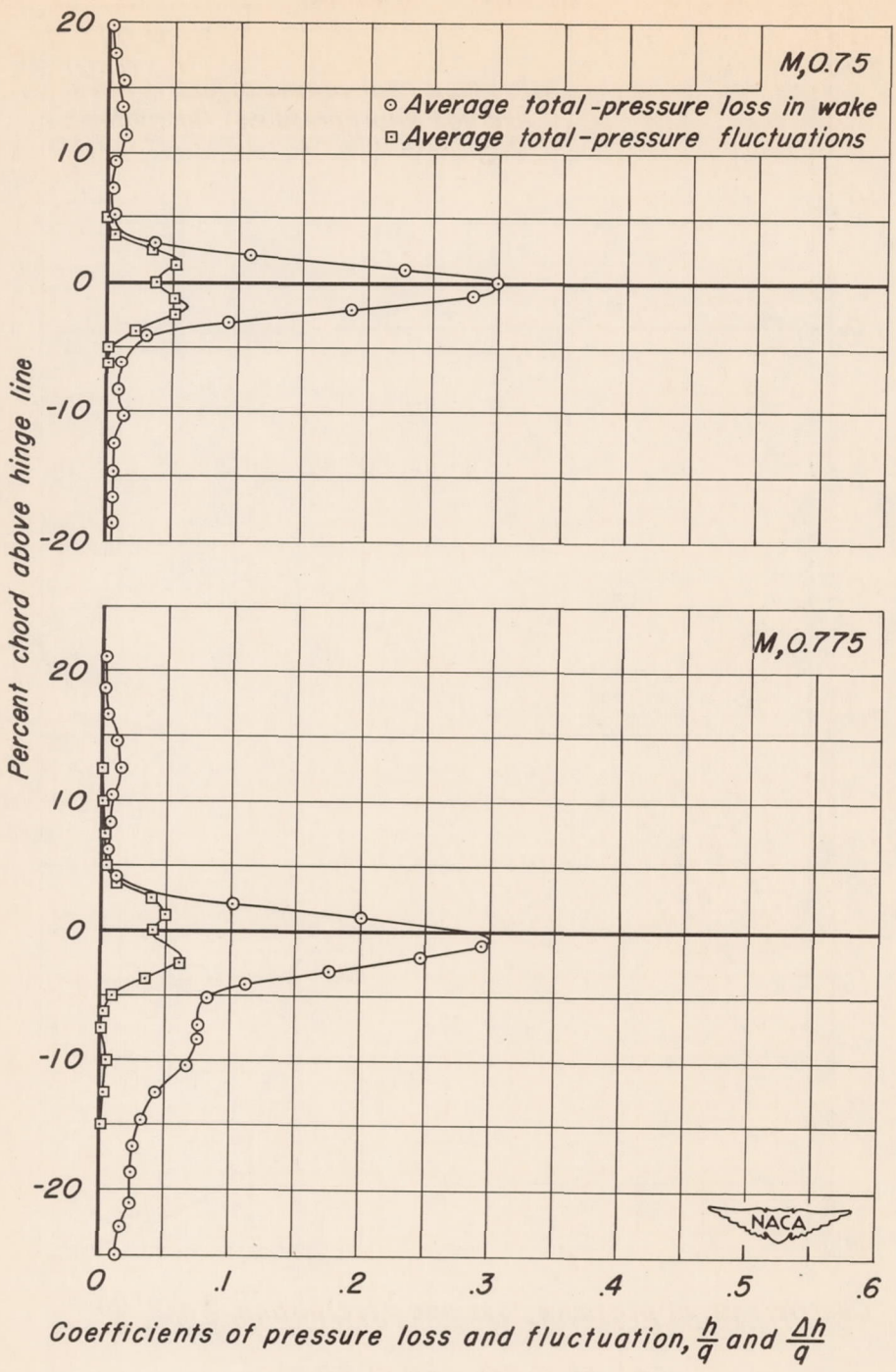

(b) M, 0.75 and 0.775

Figure 8.- Continued.

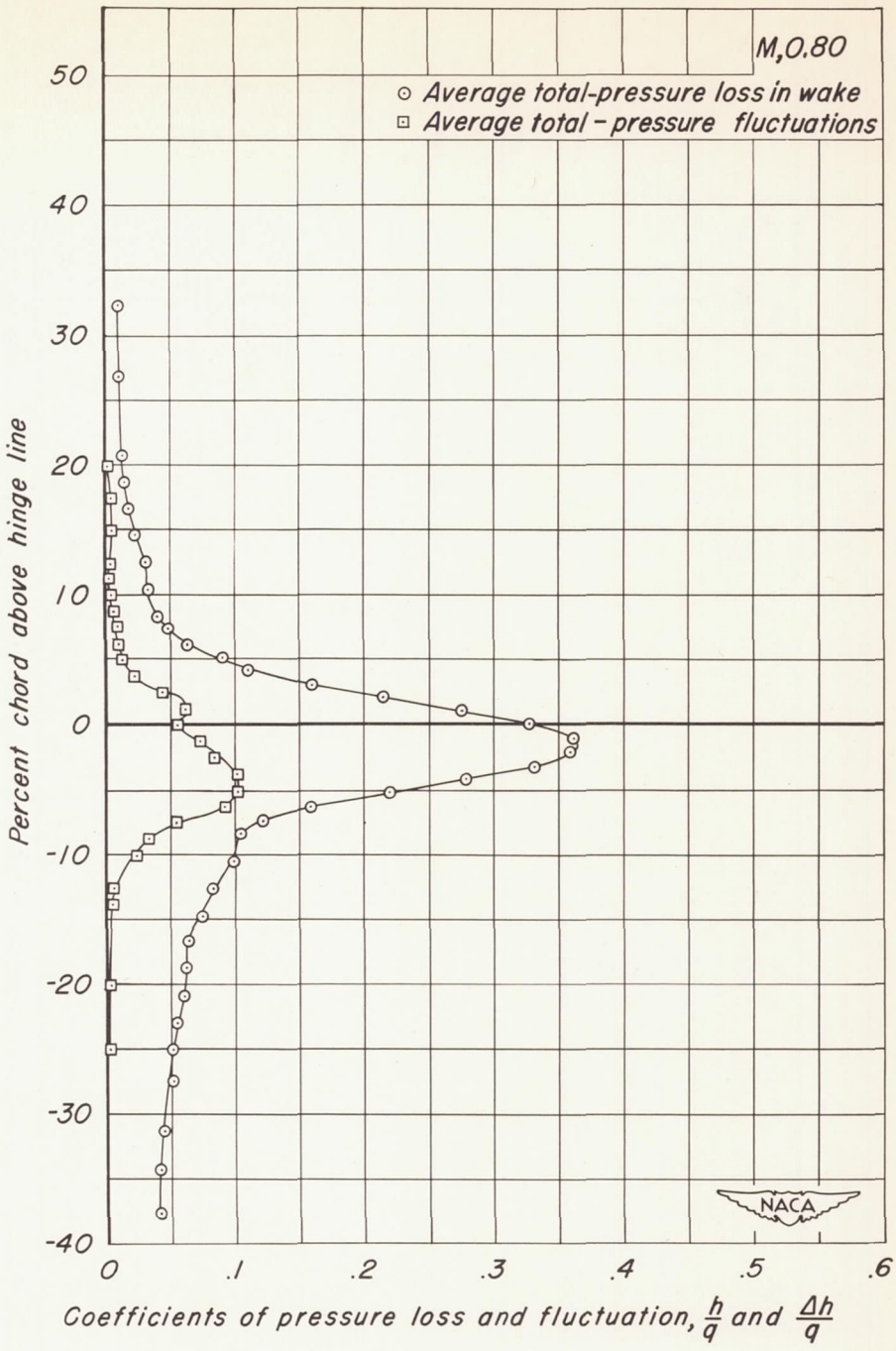

(c) M, 0.80

Figure 8.—Concluded.

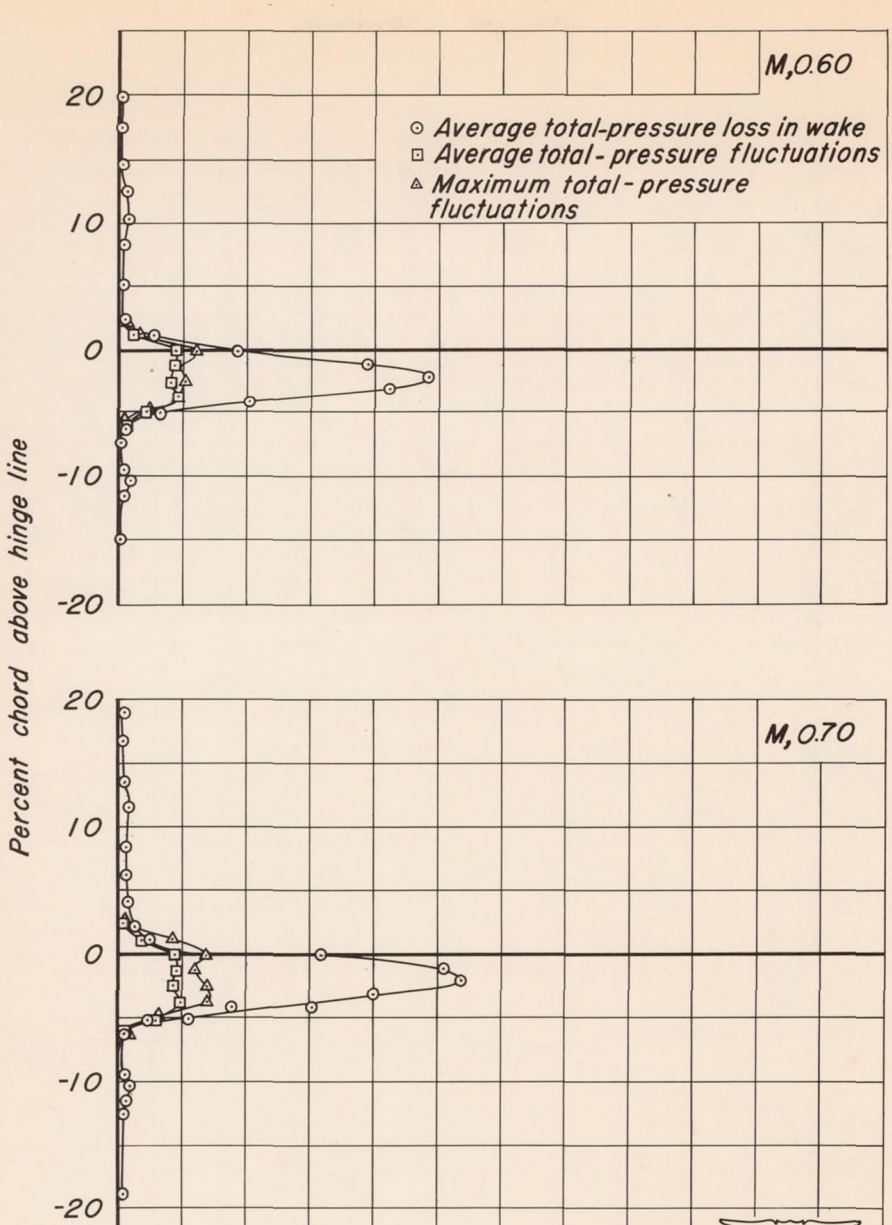

(a) M,0.60 and 0.70

Figure 9.—Wake characteristics at 70-percent-chord aft of the NACA 23013 airfoil. α,+0.°

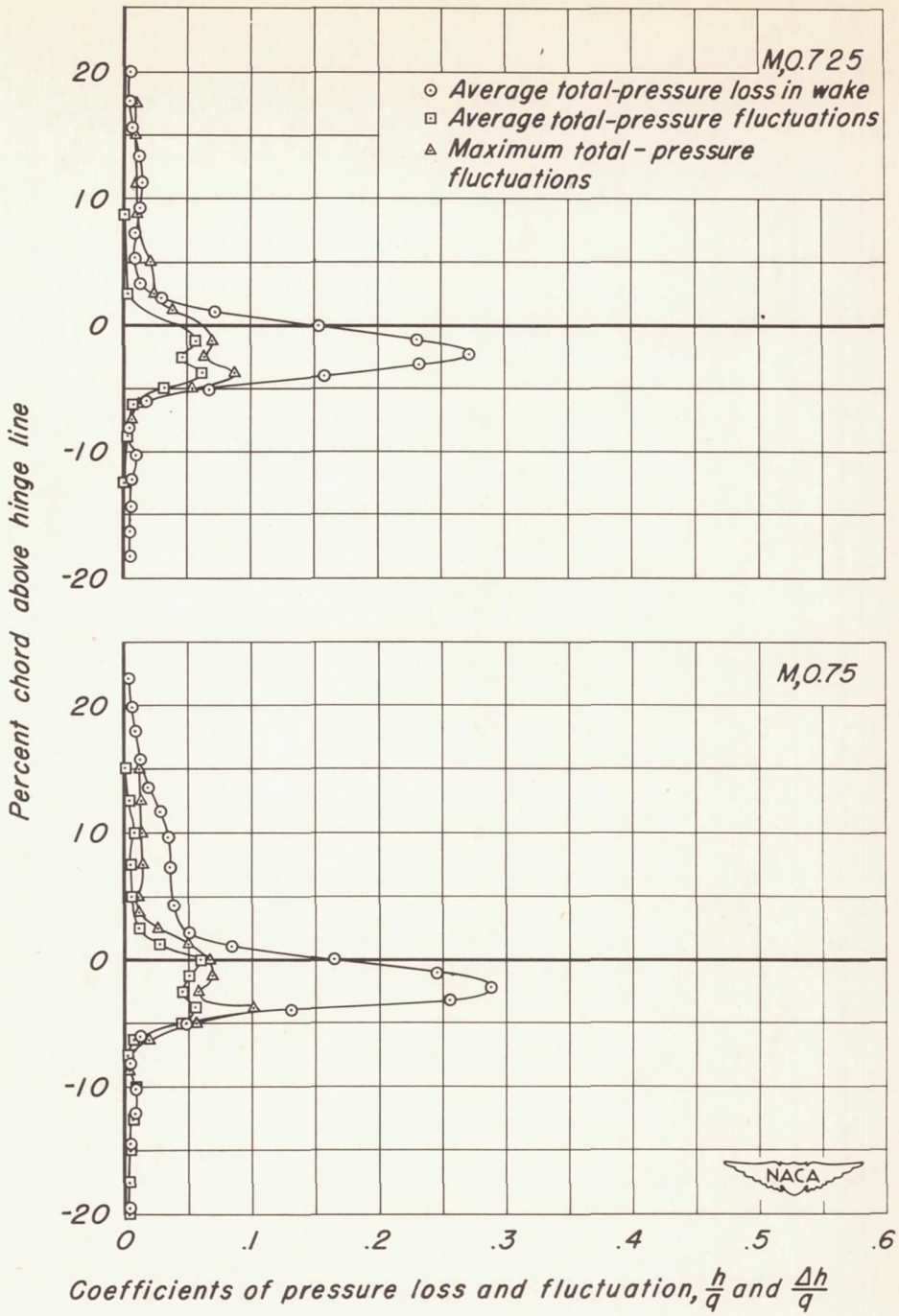

(b) M, 0.725 and 0.75

Figure 9.—Continued.

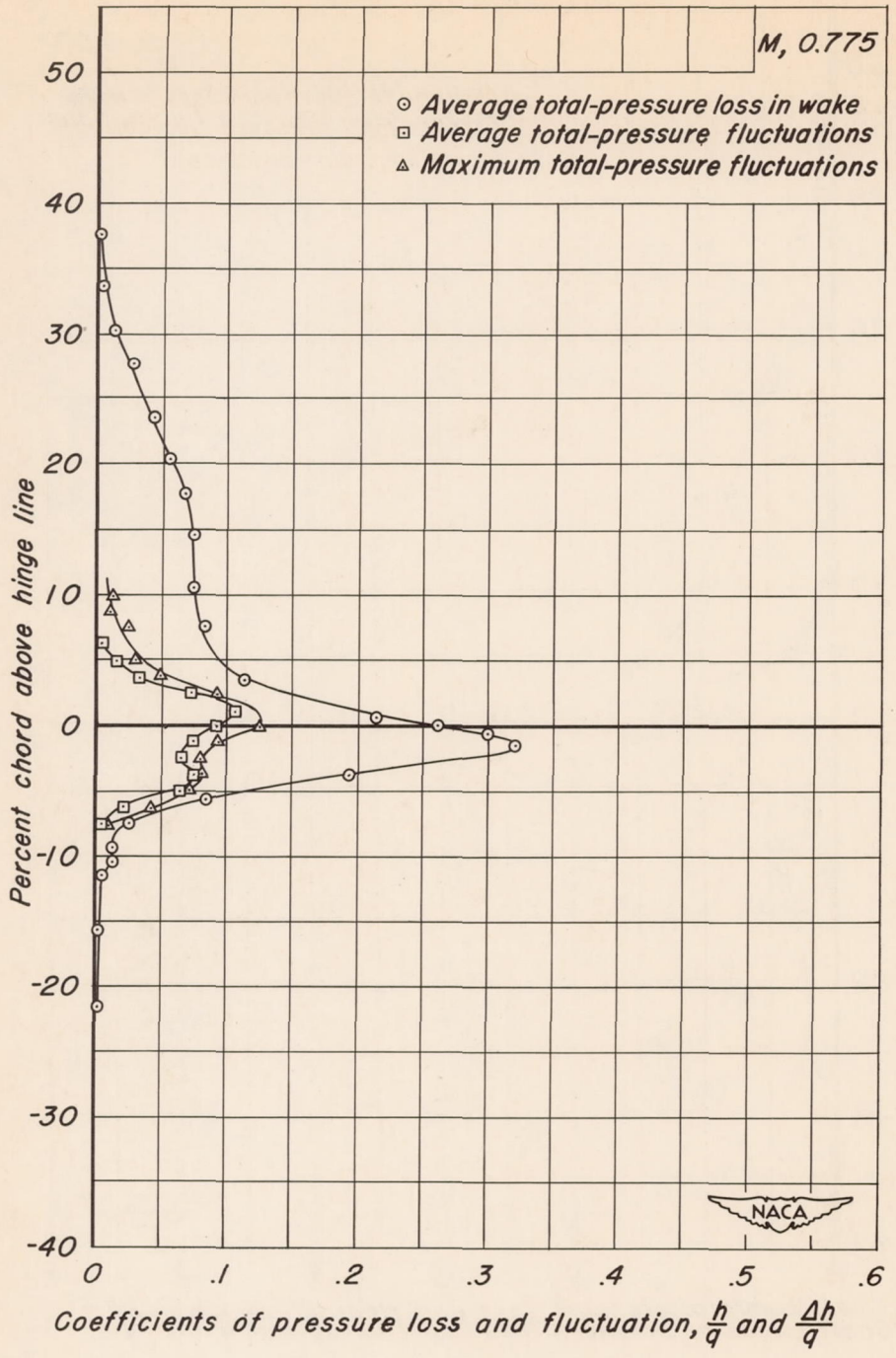

(c) M, 0.775

Figure 9.- Continued.

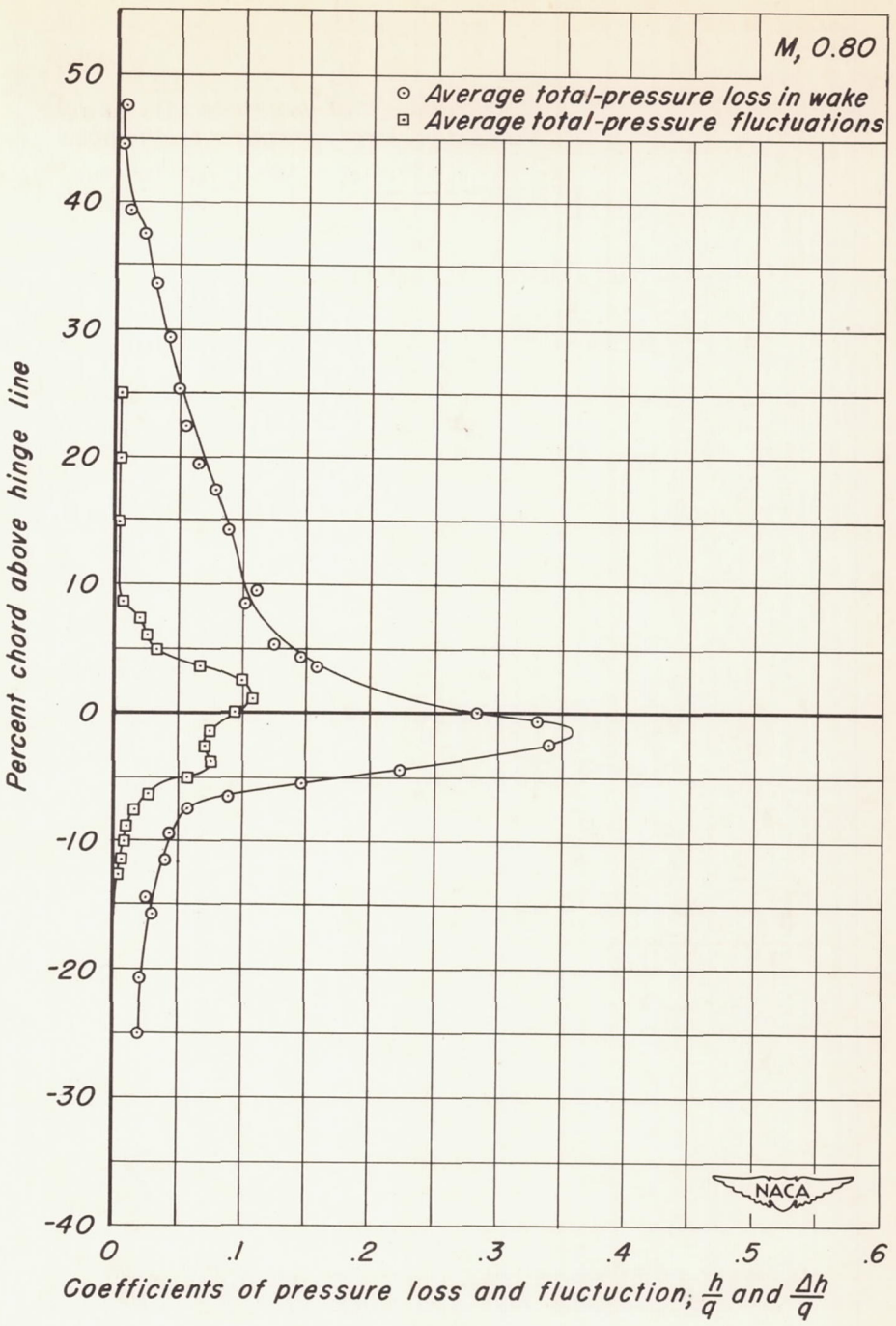

(d) M, 0.80

Figure 9.- Concluded.

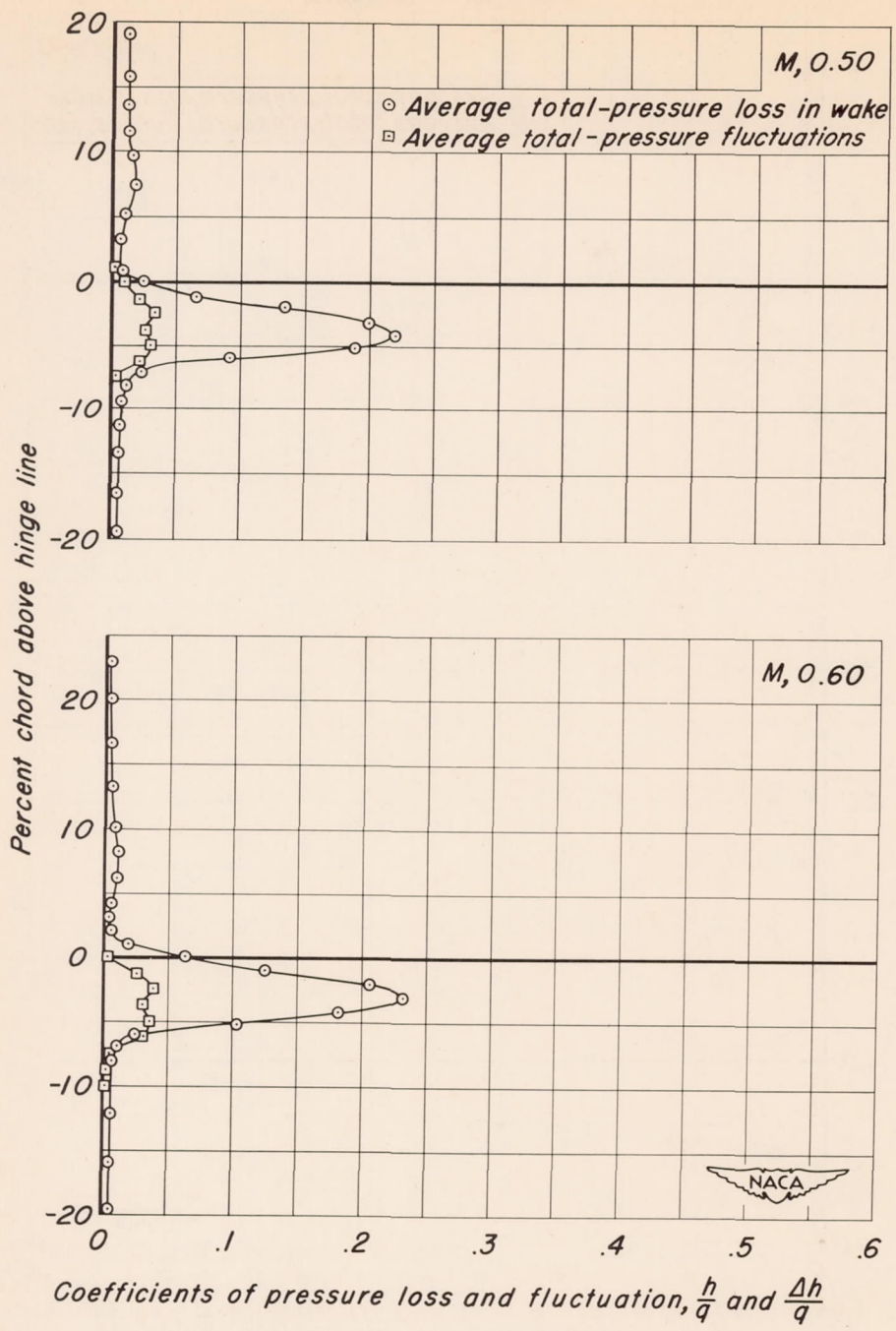

(a) M, 0.50 and 0.60

Figure 10.—Wake characteristics at 70-percent-chord aft of the NACA 23013 airfoil. α, +2°

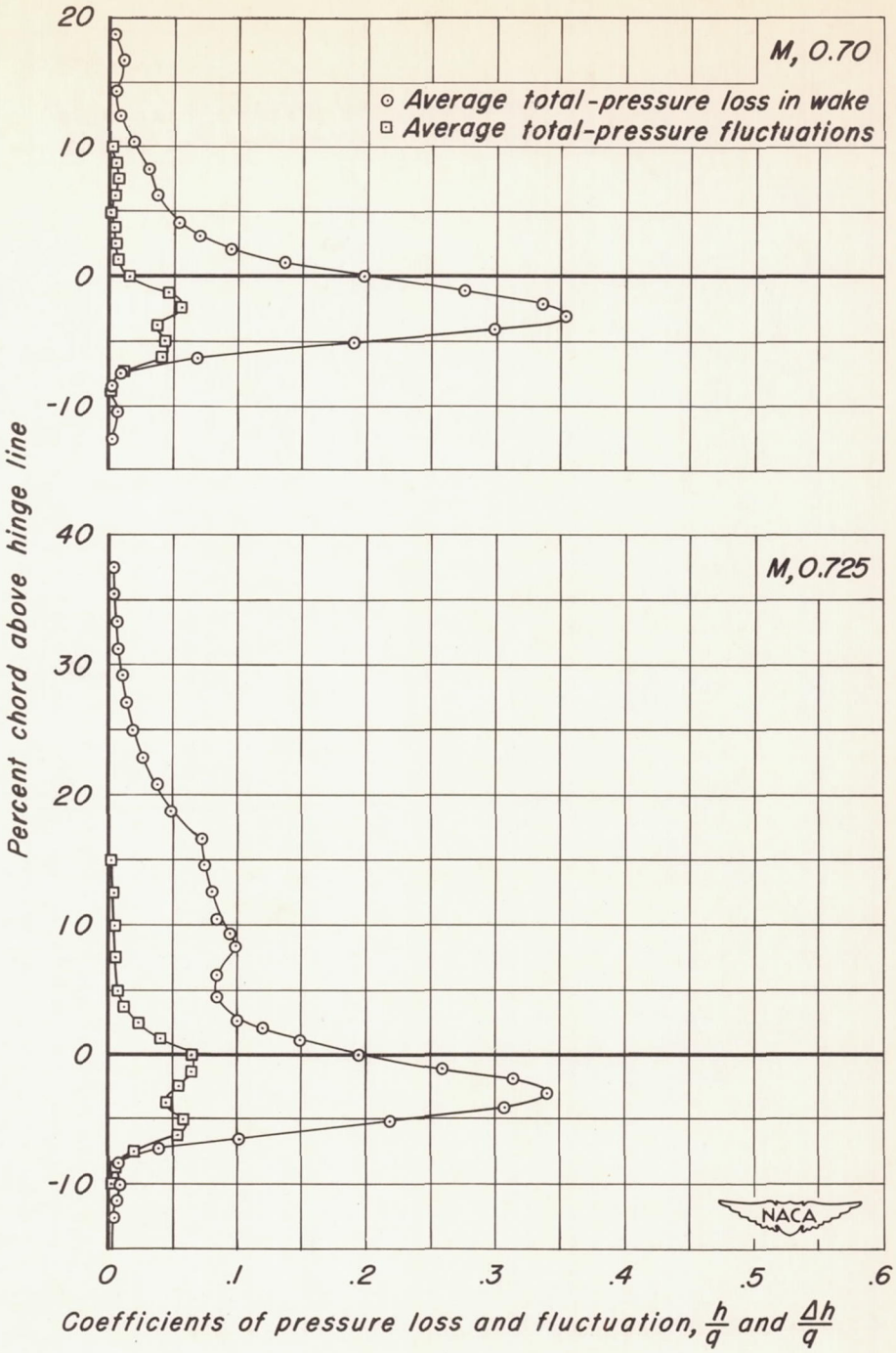

(b) M, 0.70 and 0.725

Figure 10.–Continued.

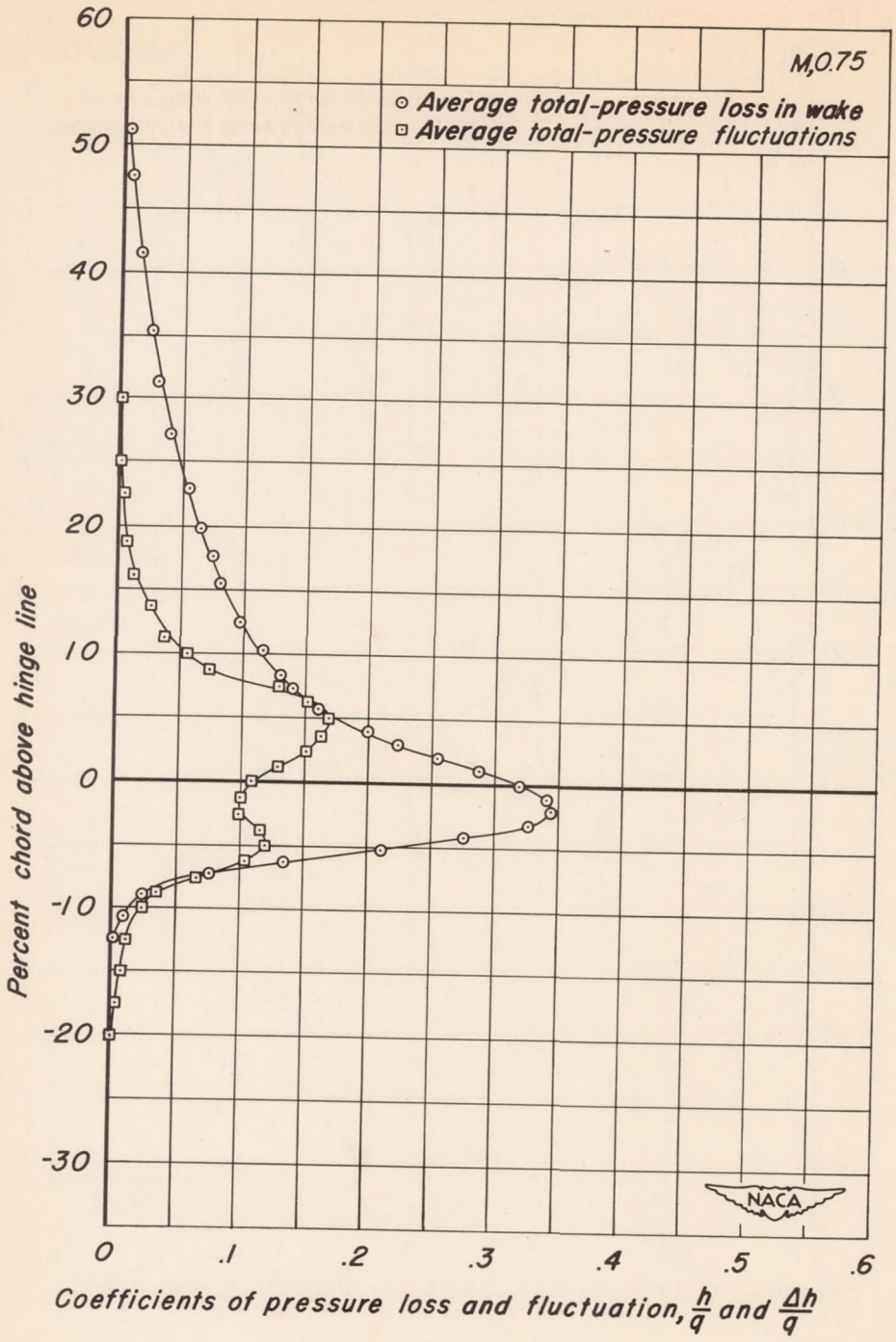

(c) M, 0.75

Figure 10.- Continued.

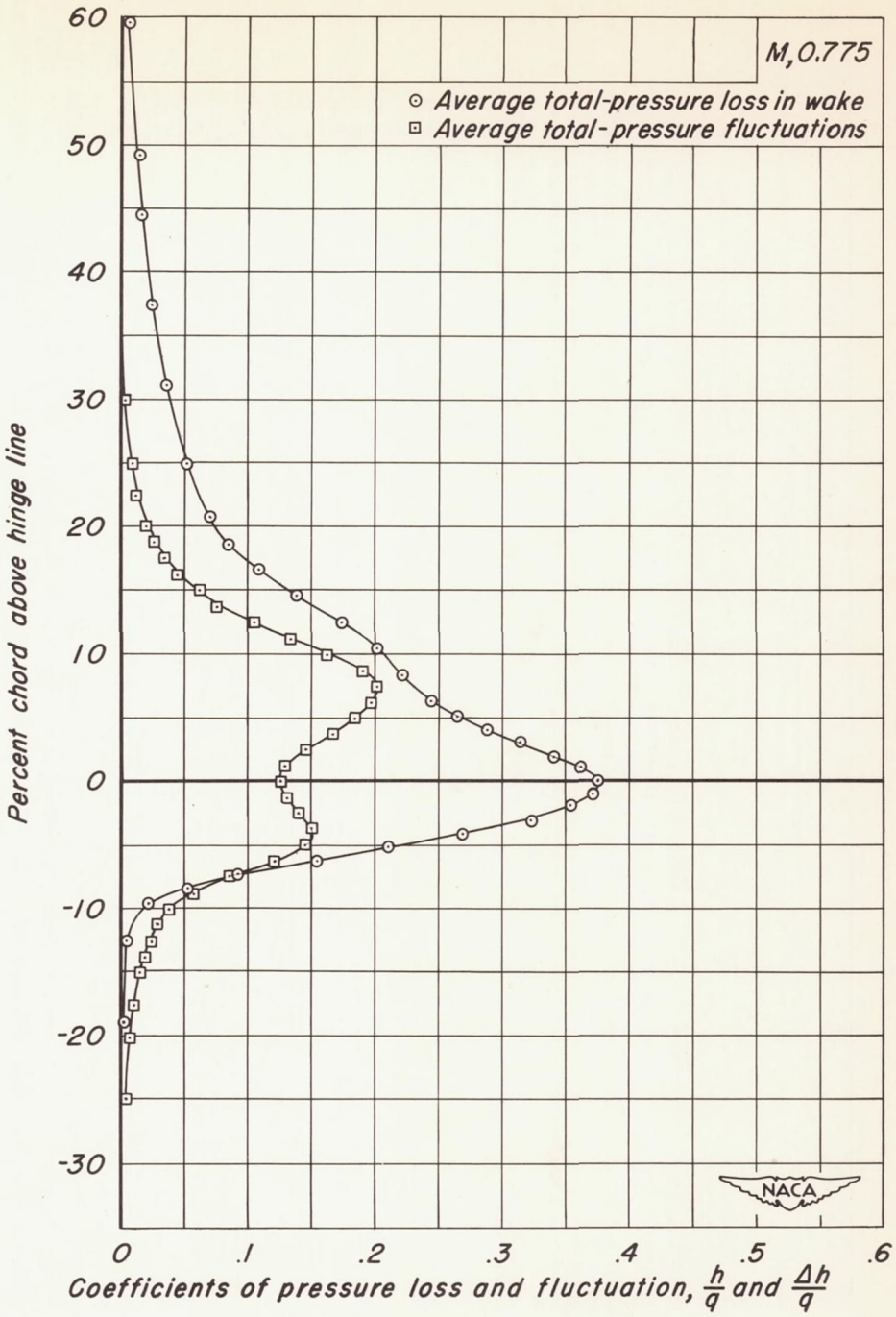

(d) M, 0.775

Figure 10.- Concluded.

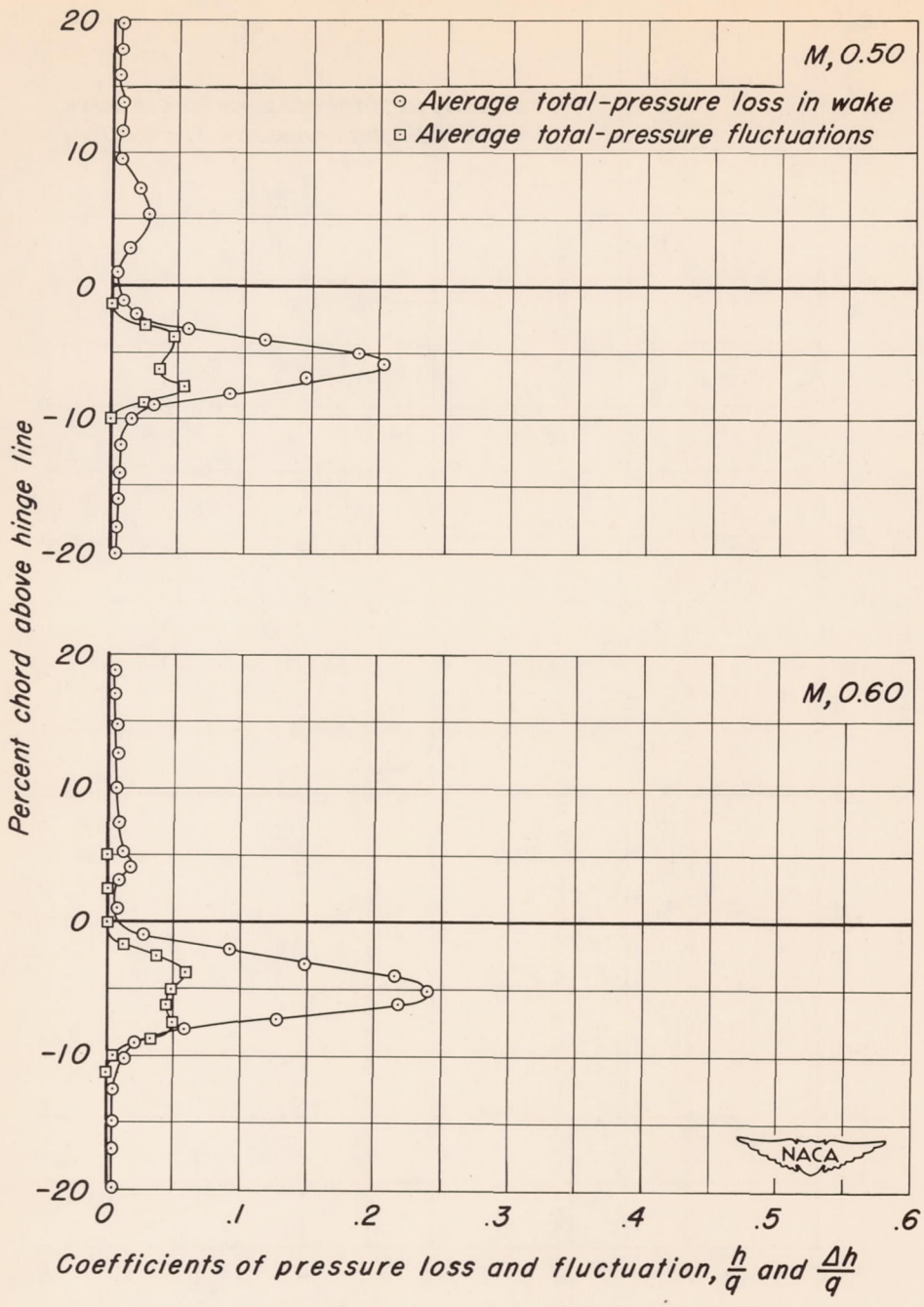

(a) M, 0.50 and 0.60

Figure 11.—Wake characteristics at 70-percent-chord aft of the NACA 23013 airfoil. α, +4°

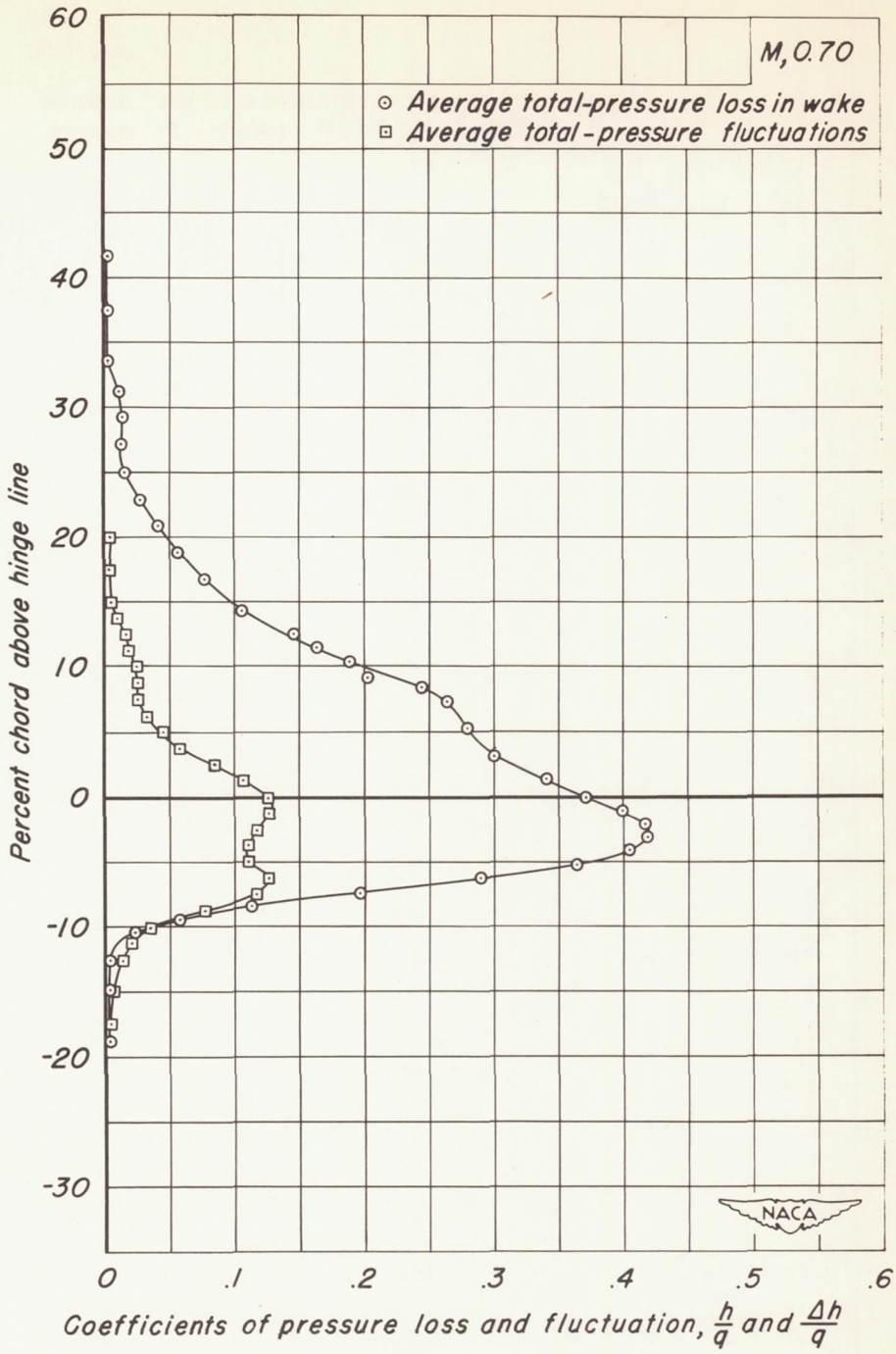

(b) M, 0.70

Figure 11.—Continued.

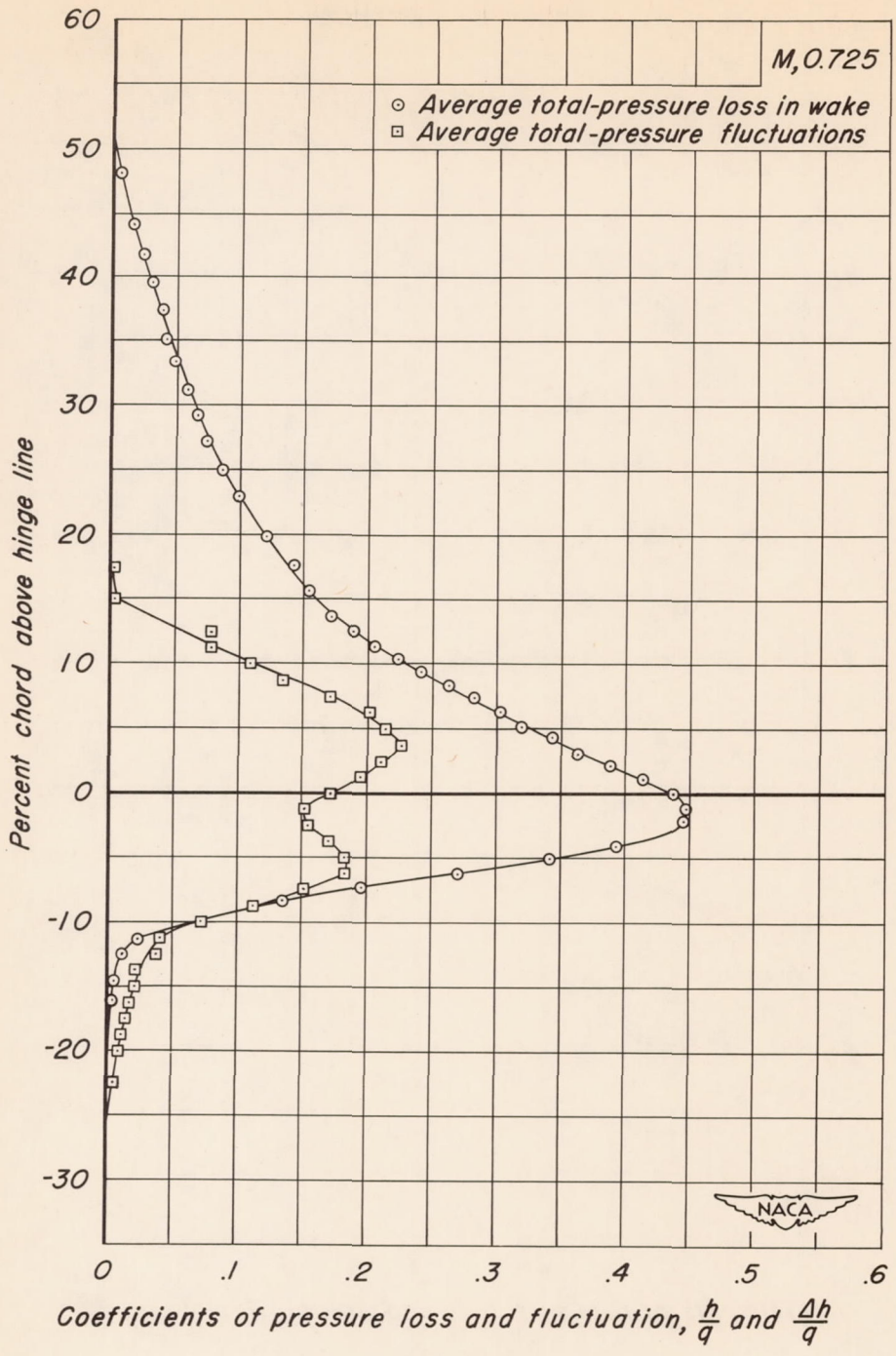

(c) M, 0.725

Figure 11.– Continued.

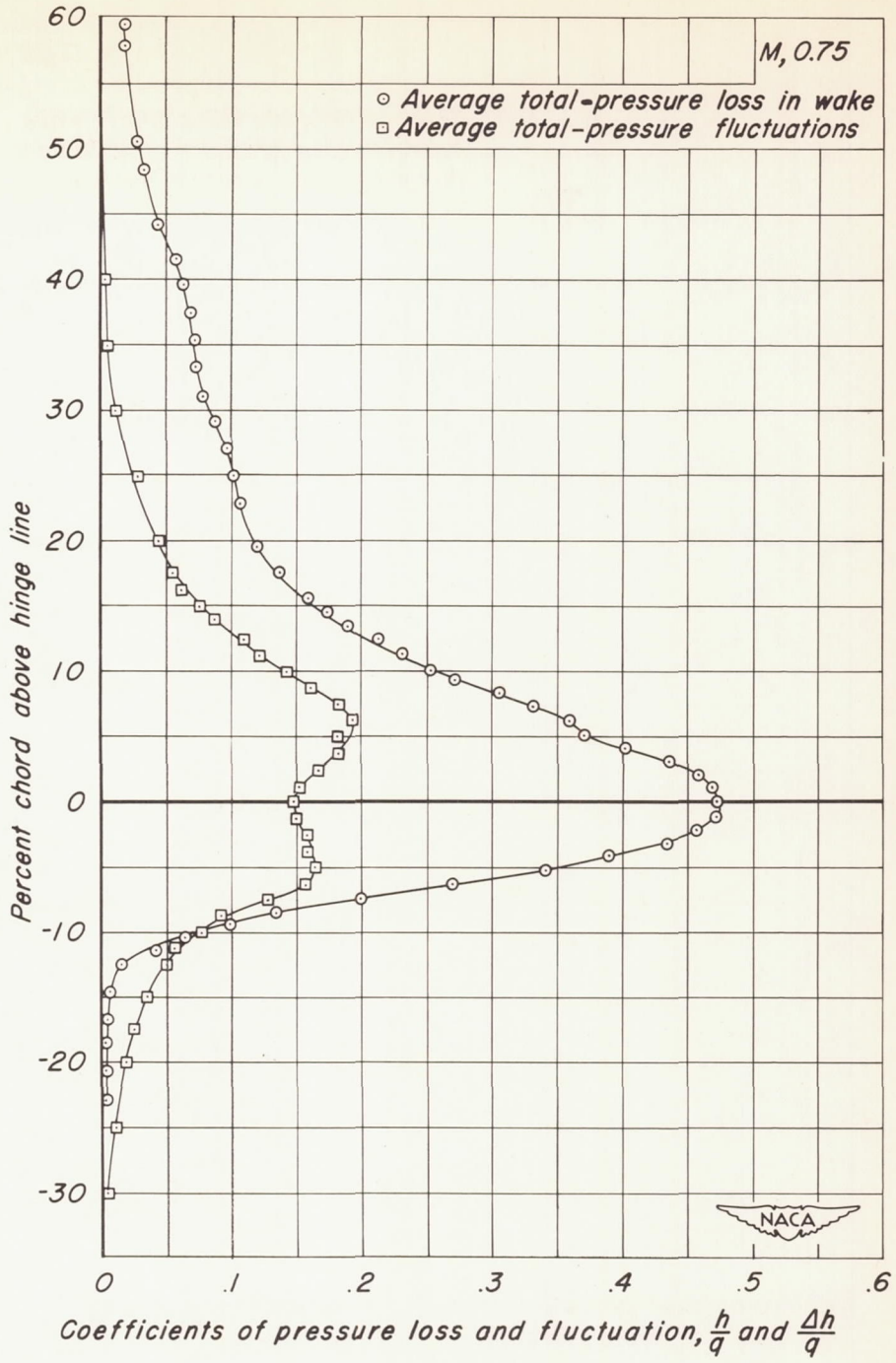

(d) M, 0.75

Figure 11.–Concluded.

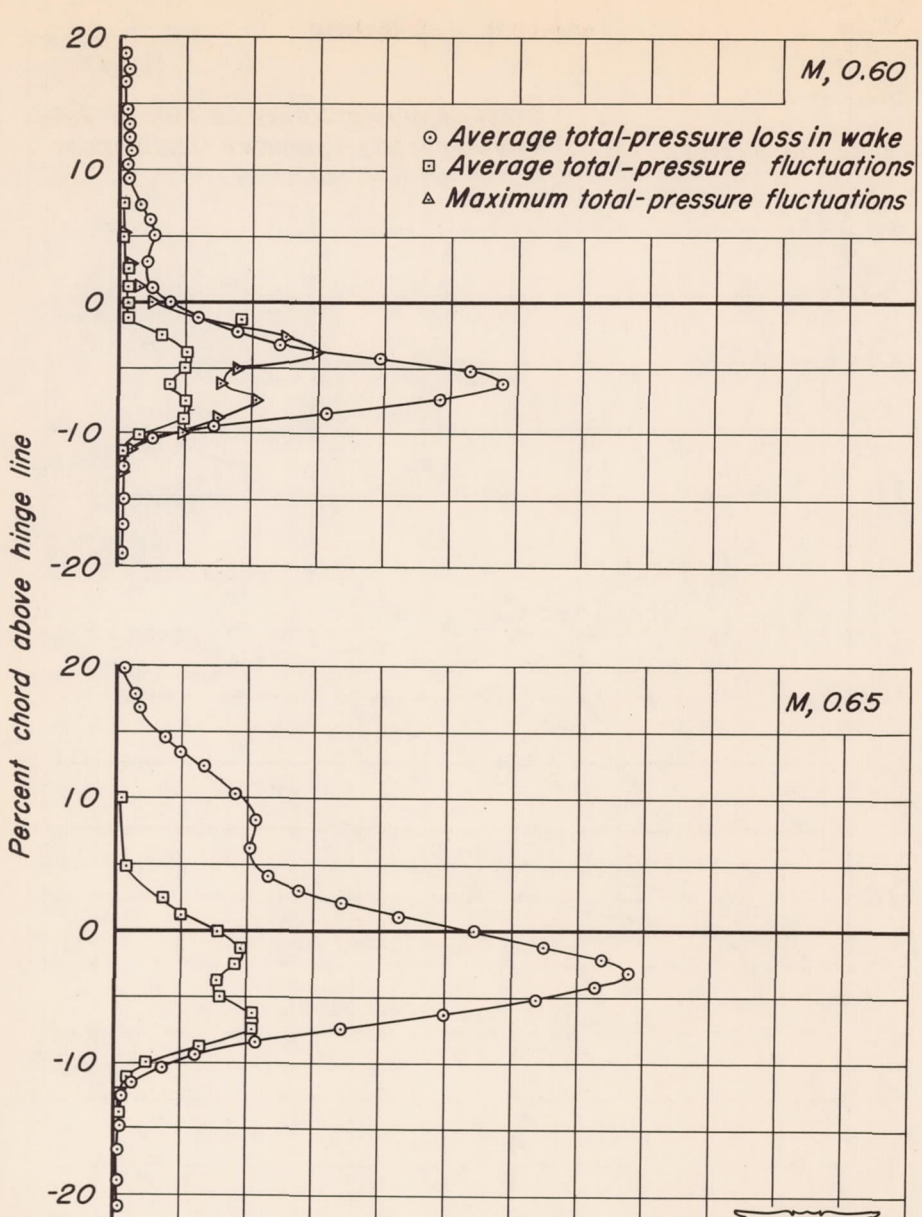

(a) M, 0.60 and 0.65

Figure 12.–Wake characteristics at 70-percent-chord aft of the NACA 23013 airfoil. α, +5°

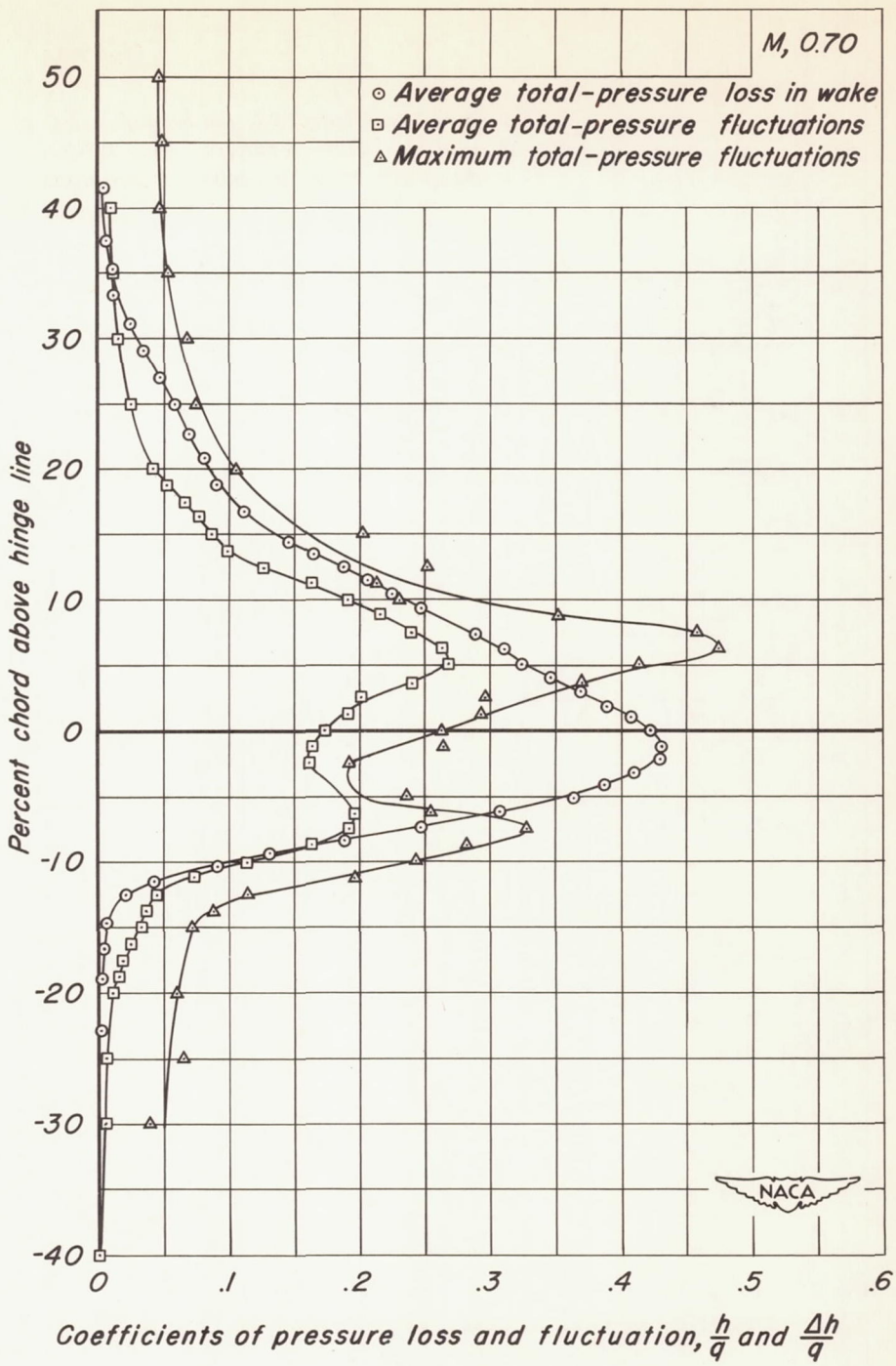

(b) M, 0.70

Figure 12.—Continued.

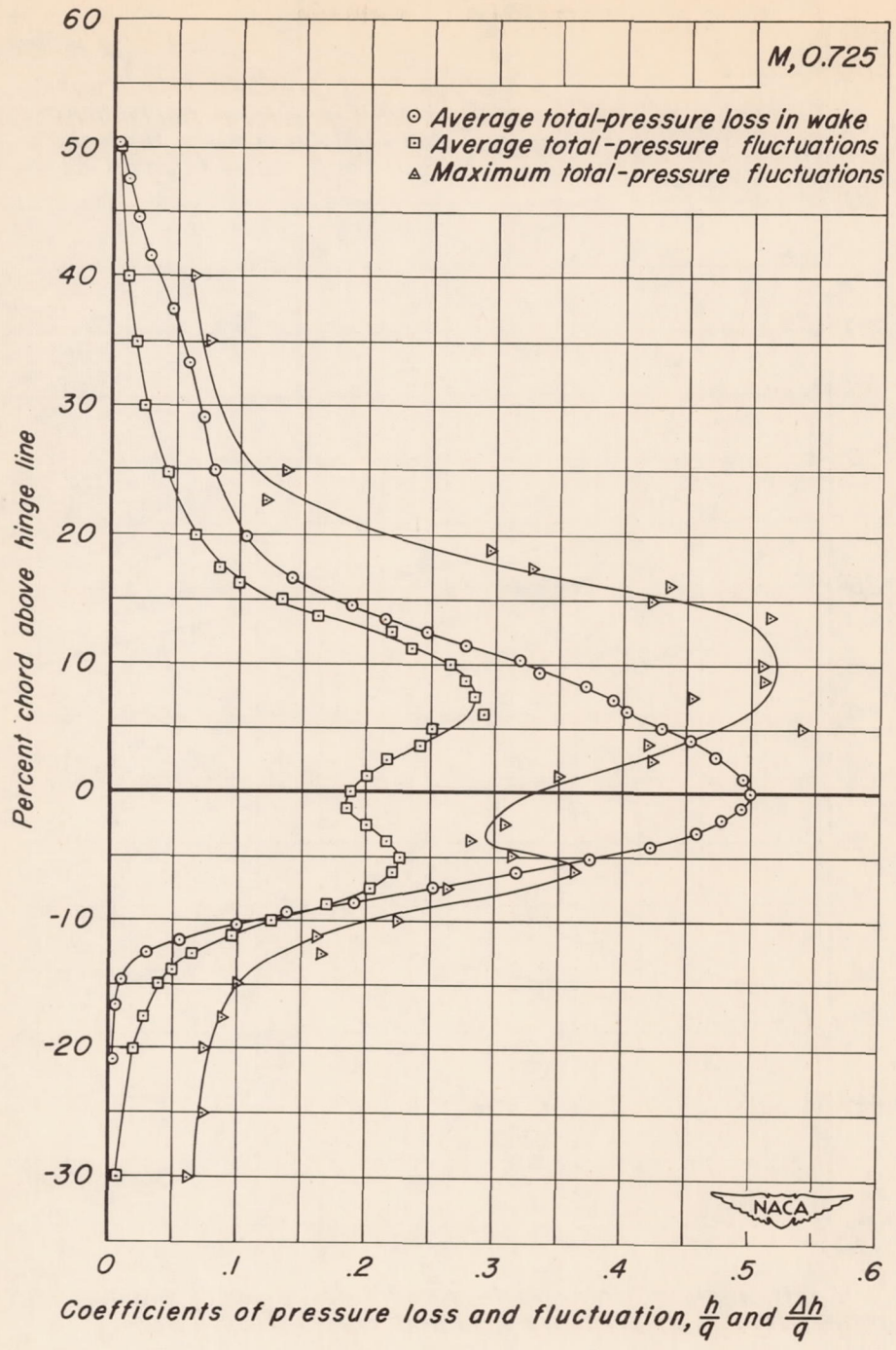

(c) M, 0.725

Figure 12.–Continued.

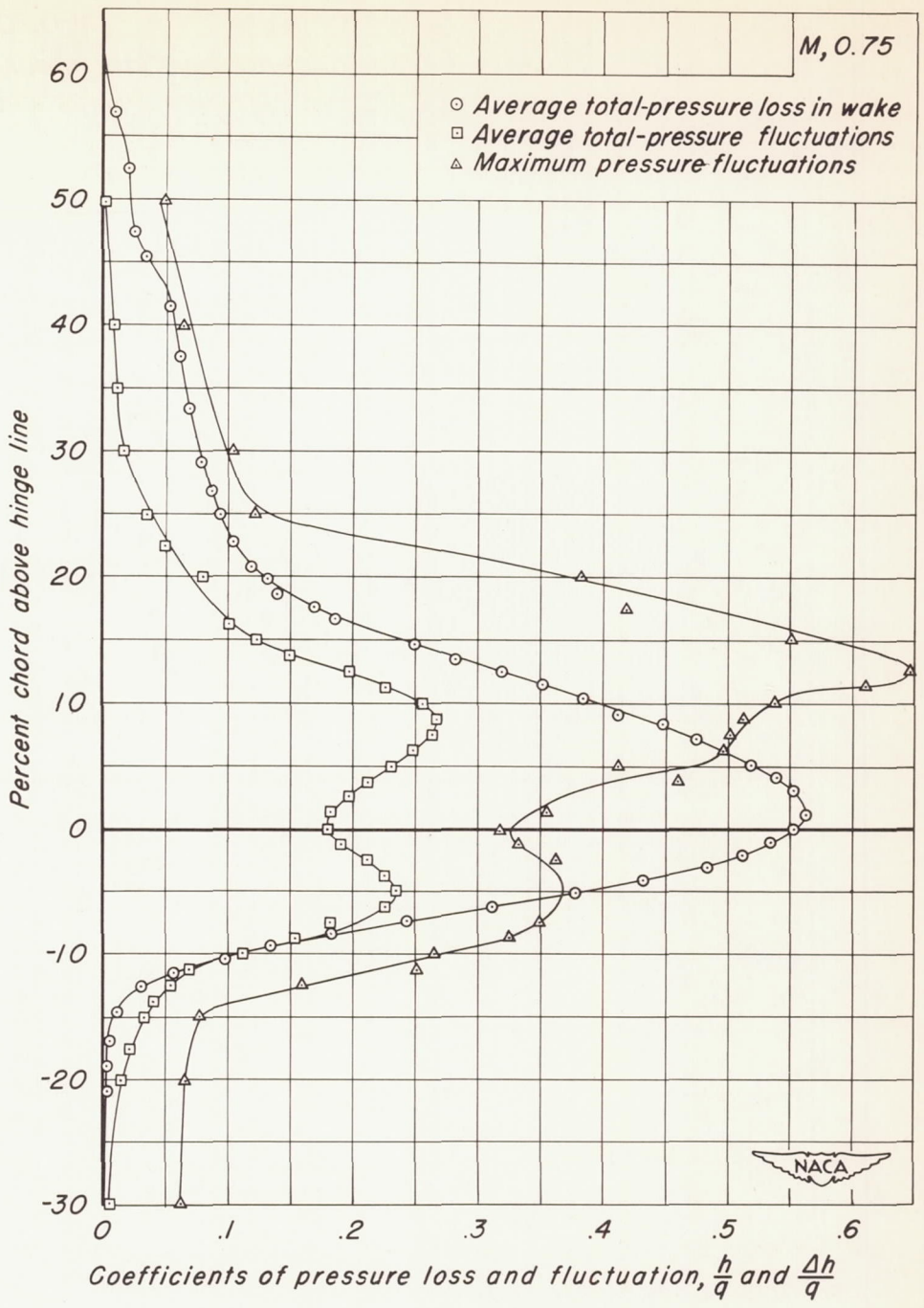

(d) M, 0.75

Figure 12.—Concluded.

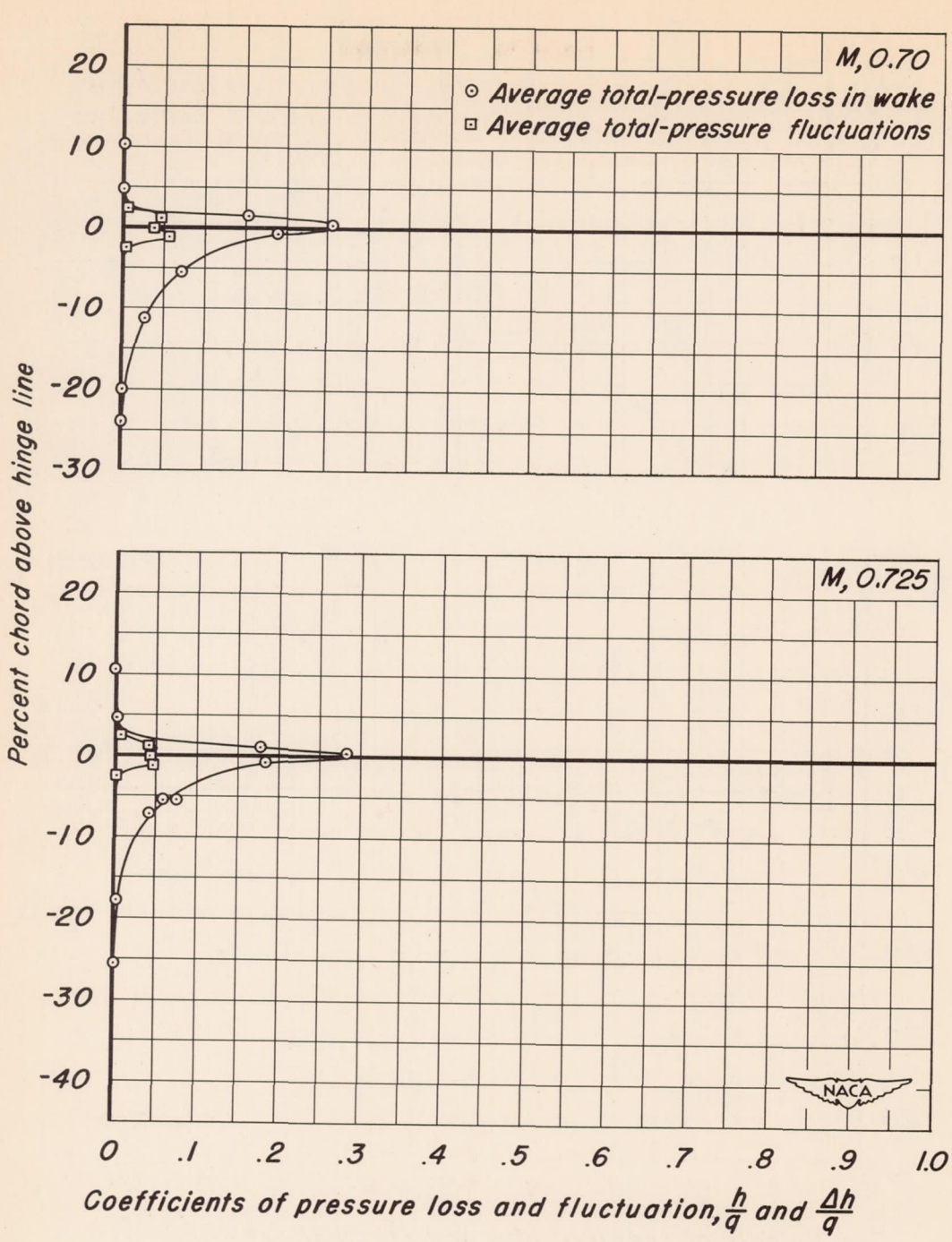

(a) M, 0.70 and 0.725

Figure 13.–Wake characteristics at 20-percent-chord aft of the NACA 23013 airfoil. α, -2°.

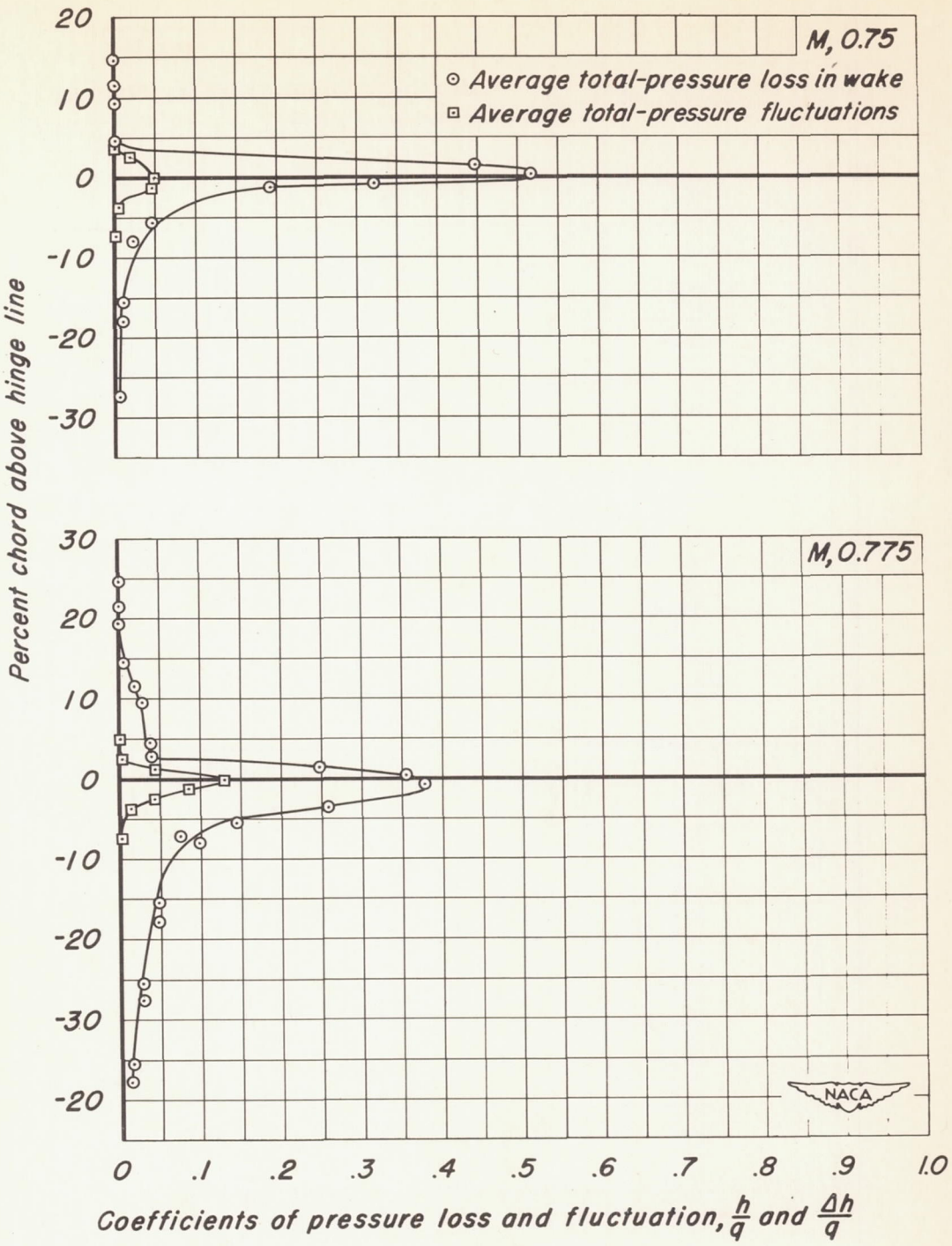

(b) M, 0.75 and 0.775

Figure 13.–Concluded.

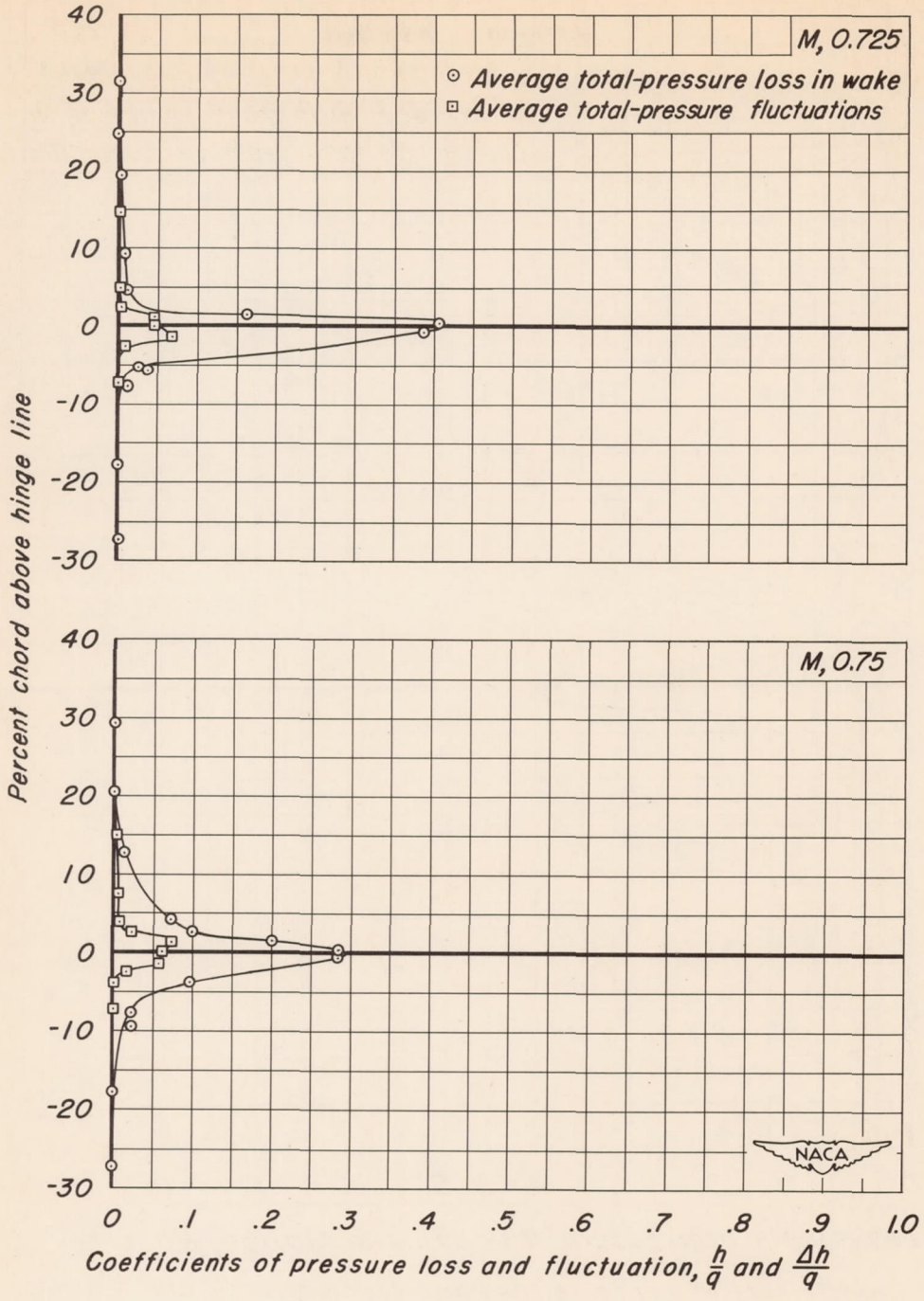

(a) M, 0.725 and 0.75

Figure 14.–Wake characteristics at 20-percent-chord aft of the NACA 23013 airfoil. α, +0°

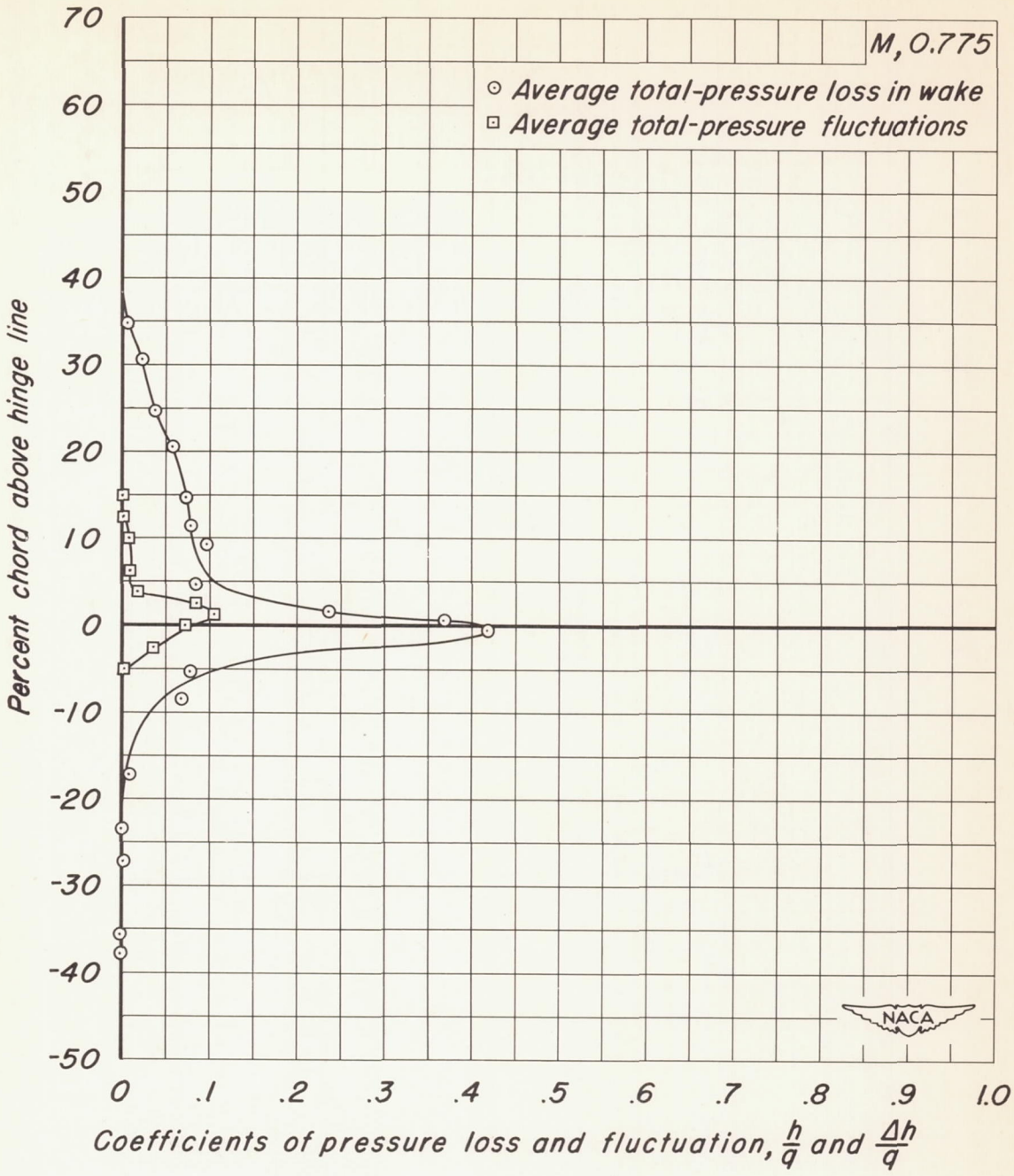

(b) M, 0.775

Figure 14.–Concluded.

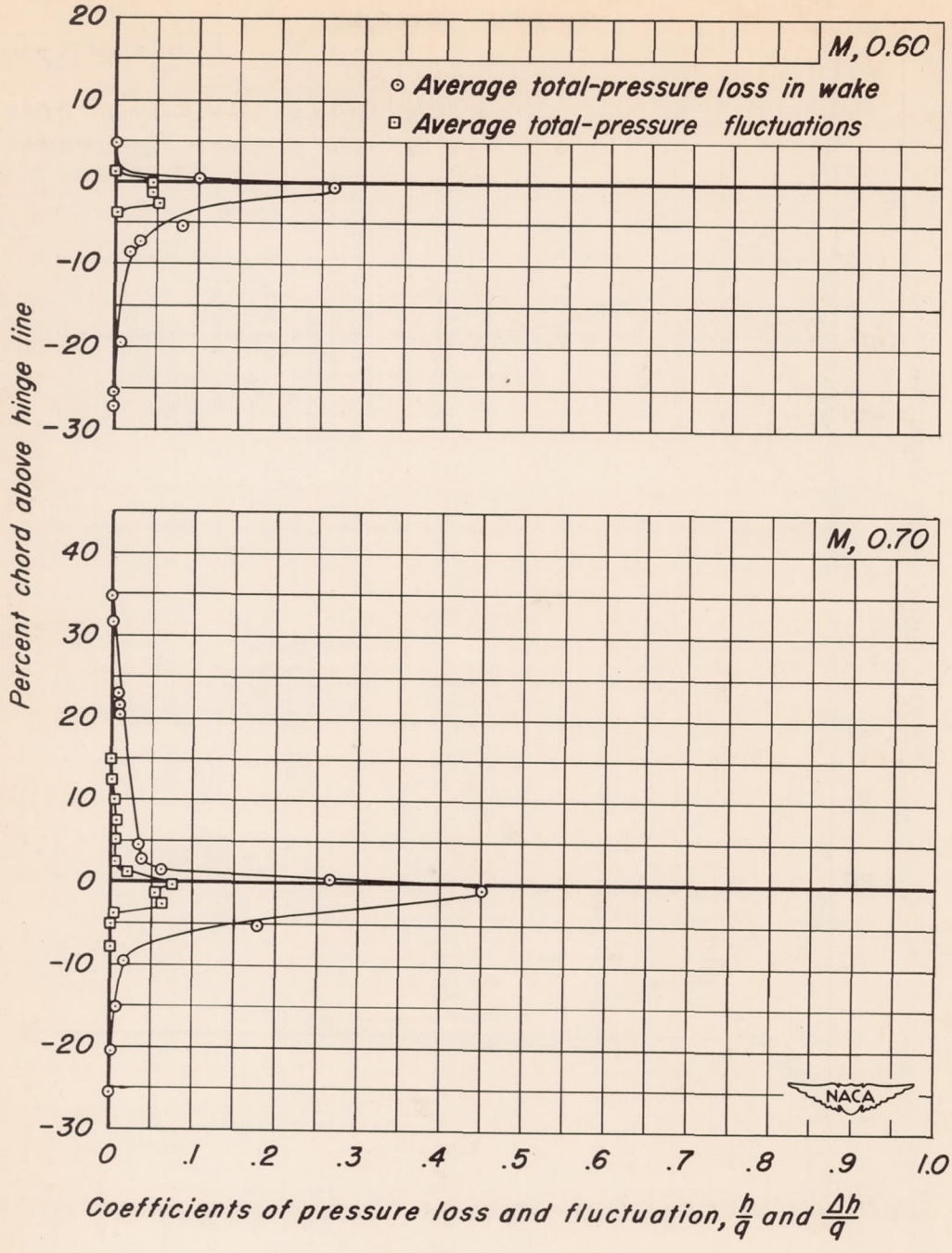

(a) M, 0.60 and 0.70

Figure 15.–Wake characteristics at 20-percent-chord aft of the NACA 23013 airfoil. α, +2°

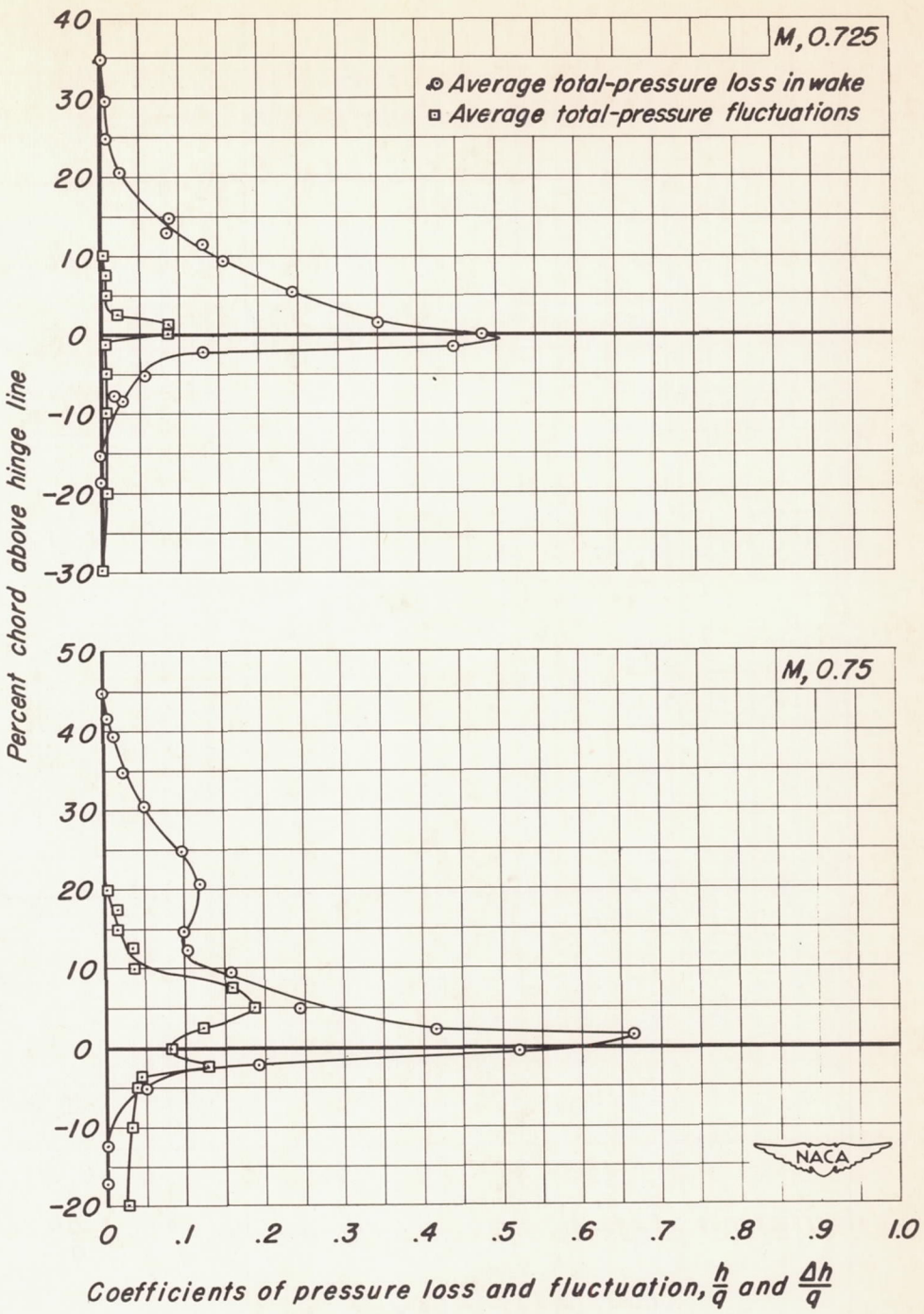

(b) M, 0.725 and 0.75

Figure 15.–Continued.

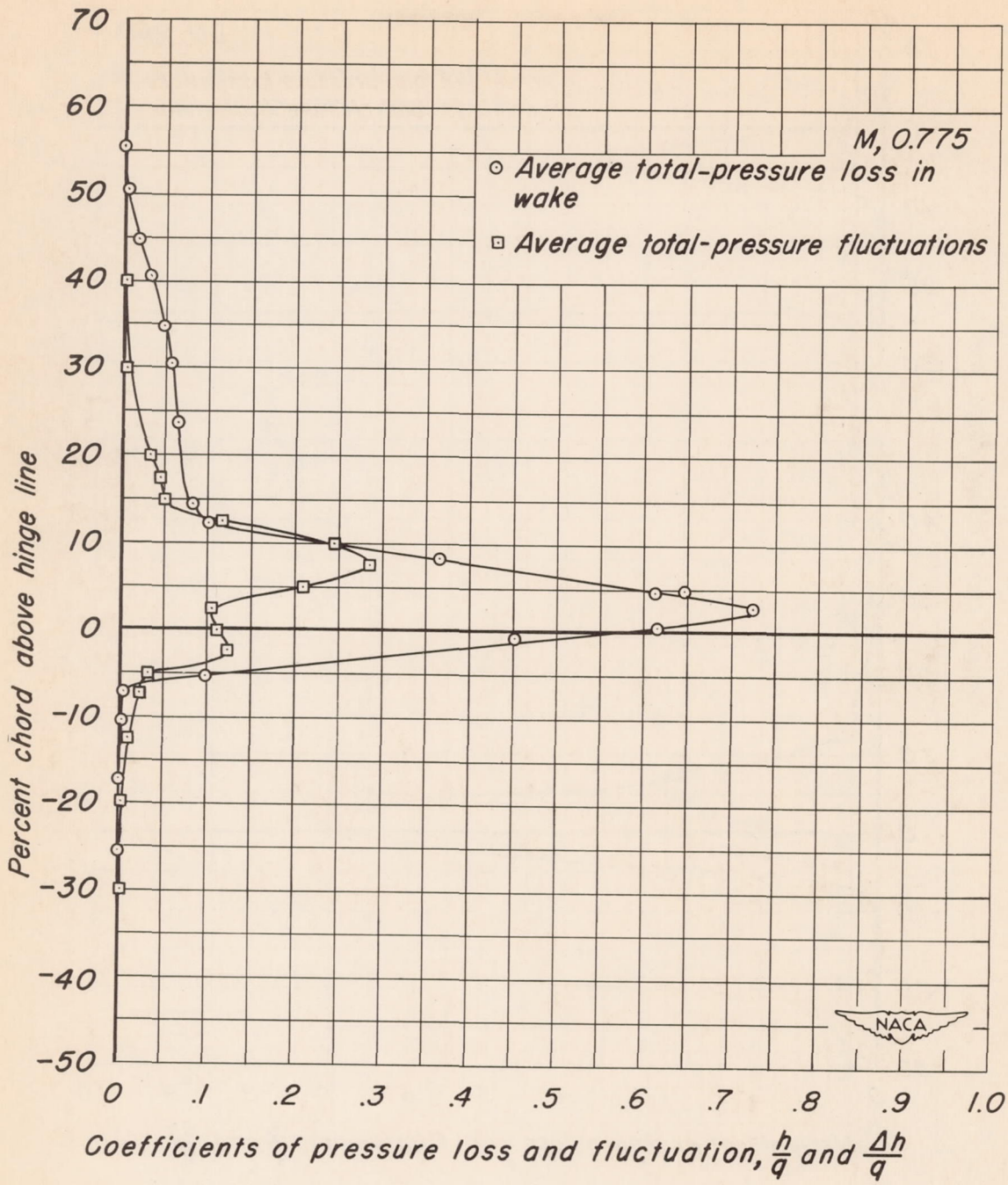

(c) M, 0.775

Figure 15.–Concluded.

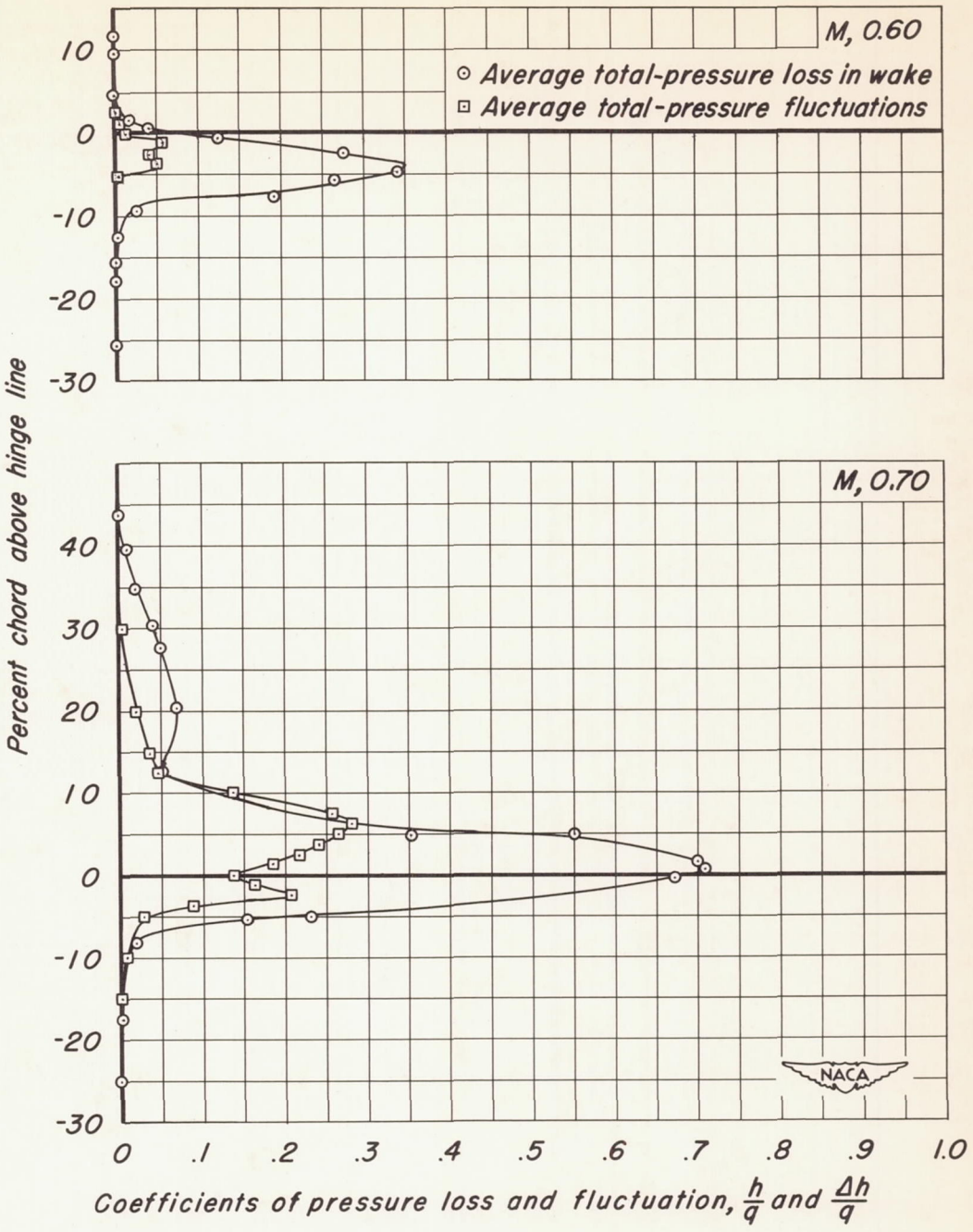

(a) M, 0.60 and 0.70

Figure 16.–Wake characteristics at 20-percent-chord aft of the NACA 23013 airfoil. α, +4°

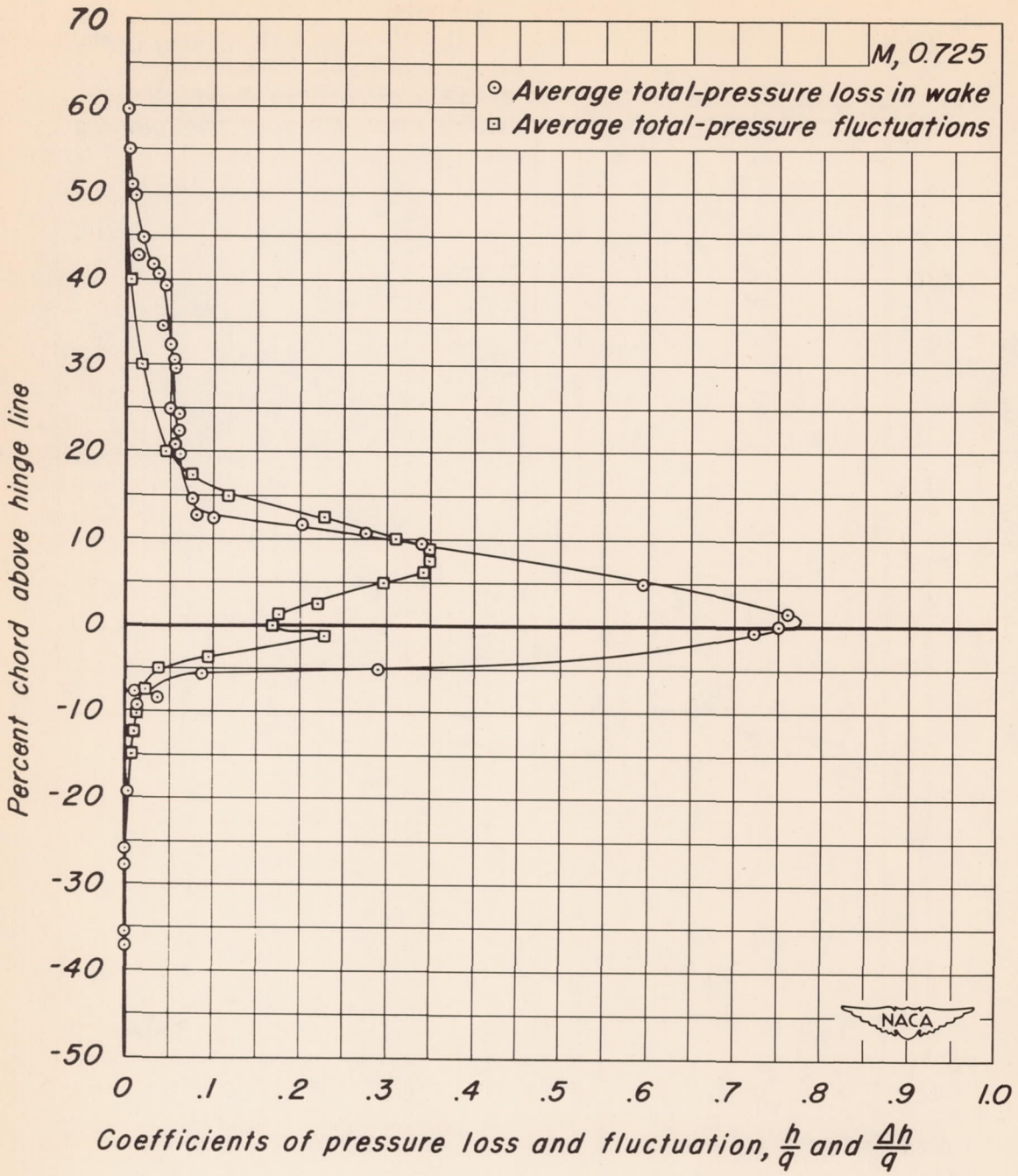

(b) M, 0.725

Figure 16.–Continued.

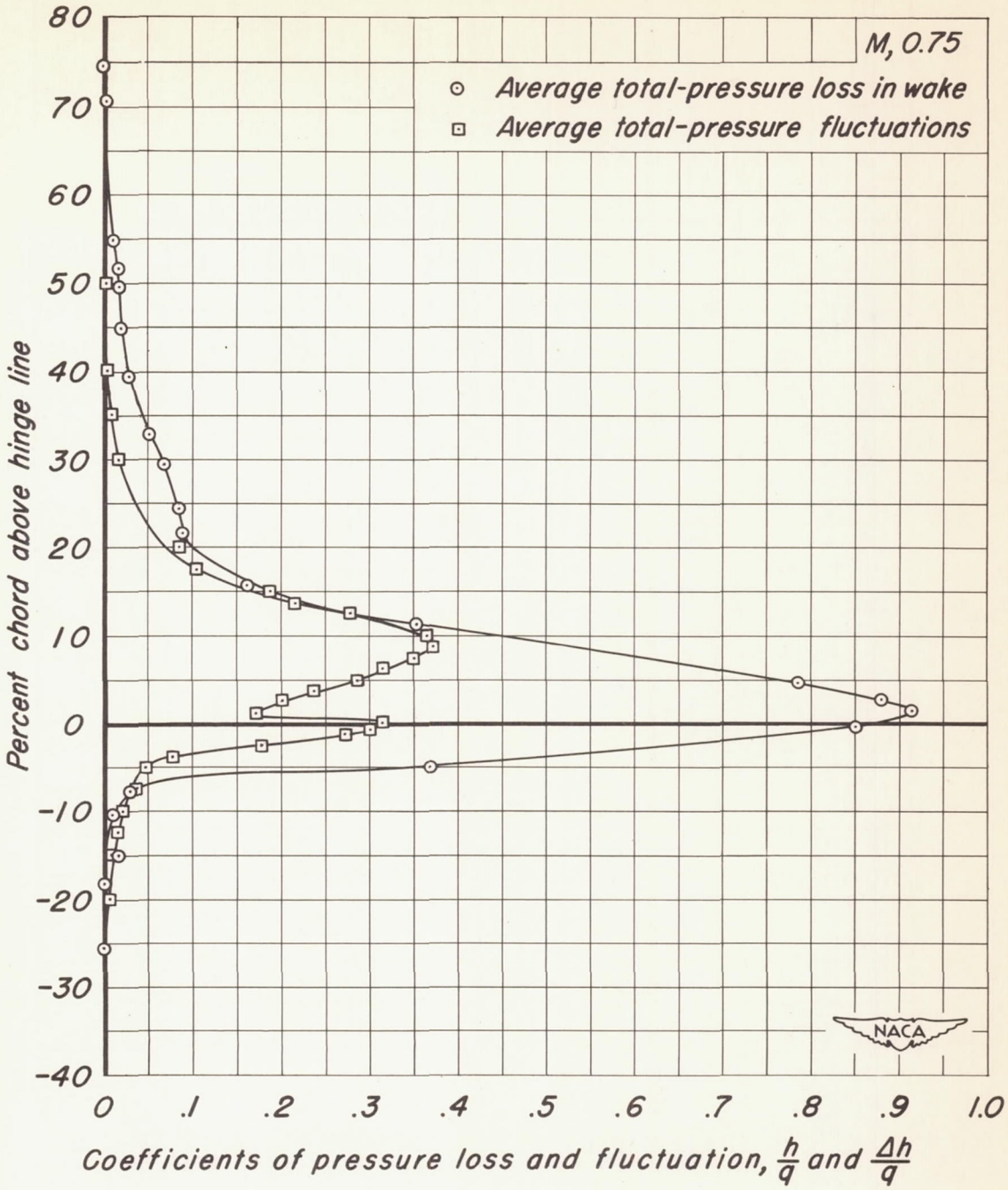

(c) M, 0.75

Figure 16.–Concluded.

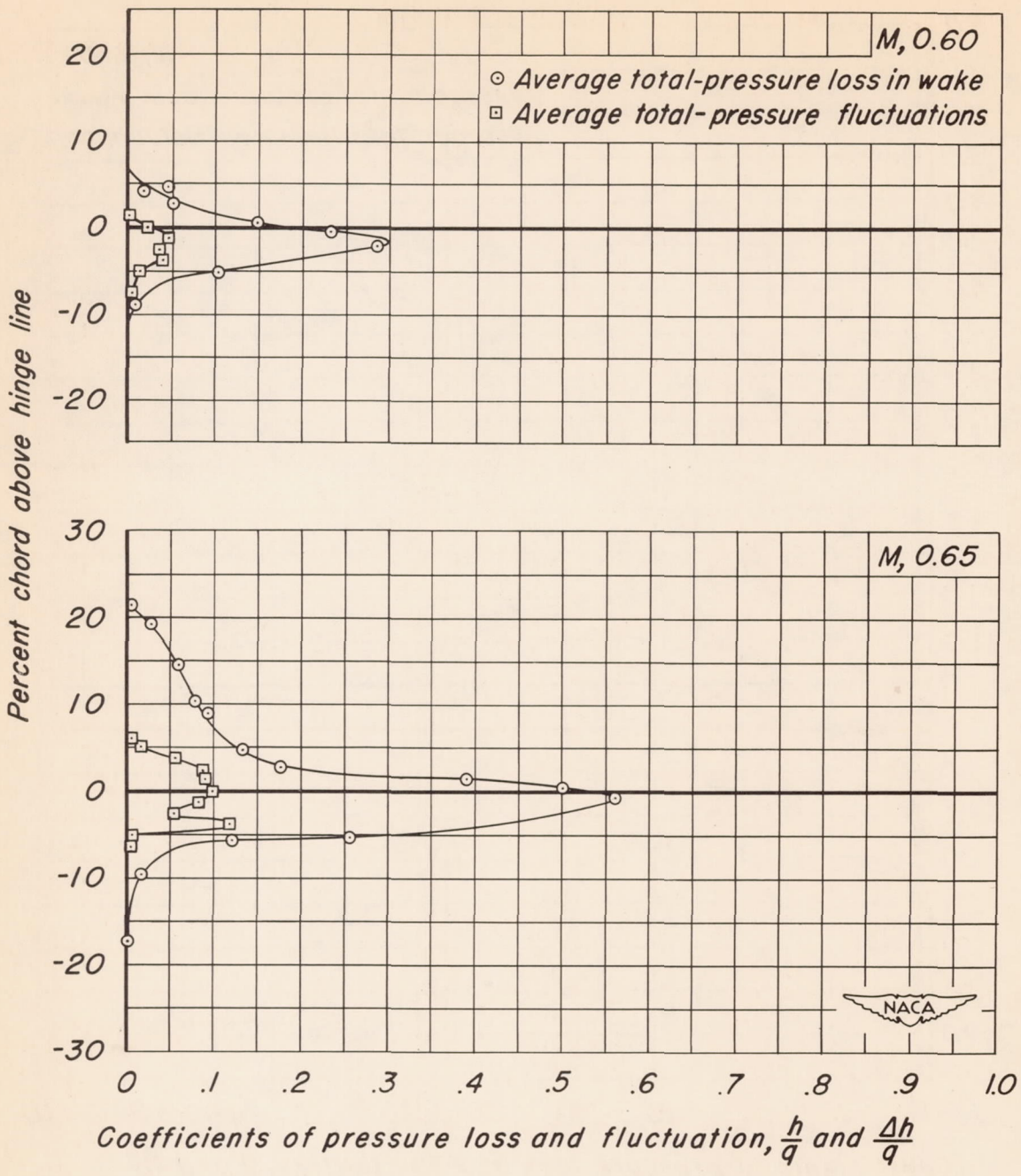

(a) M, 0.60 and 0.65

Figure 17.—Wake characteristics at 20-percent-chord aft of the NACA 23013 airfoil. α, +5°.

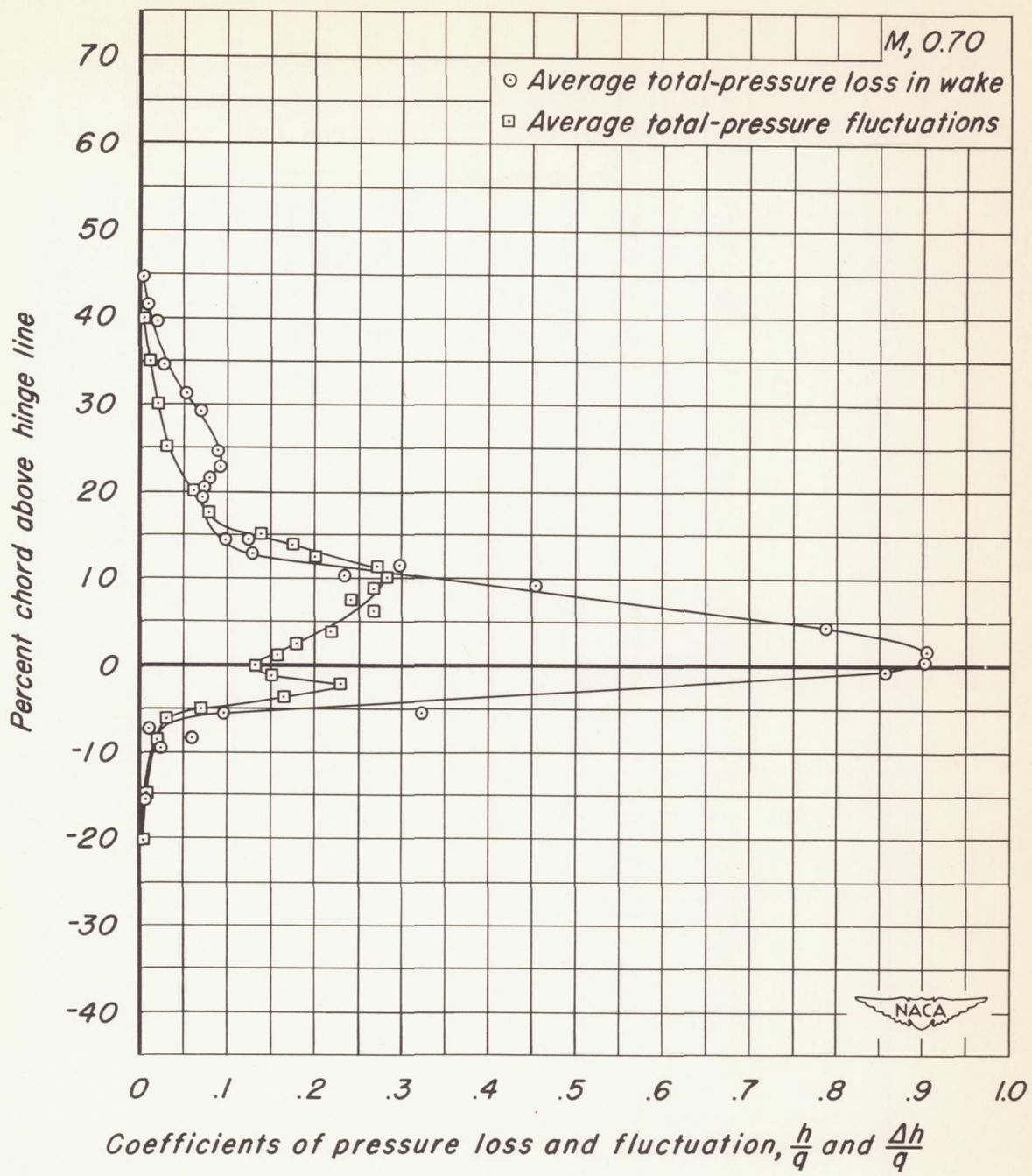

(b) M, 0.70

Figure 17.– Continued.

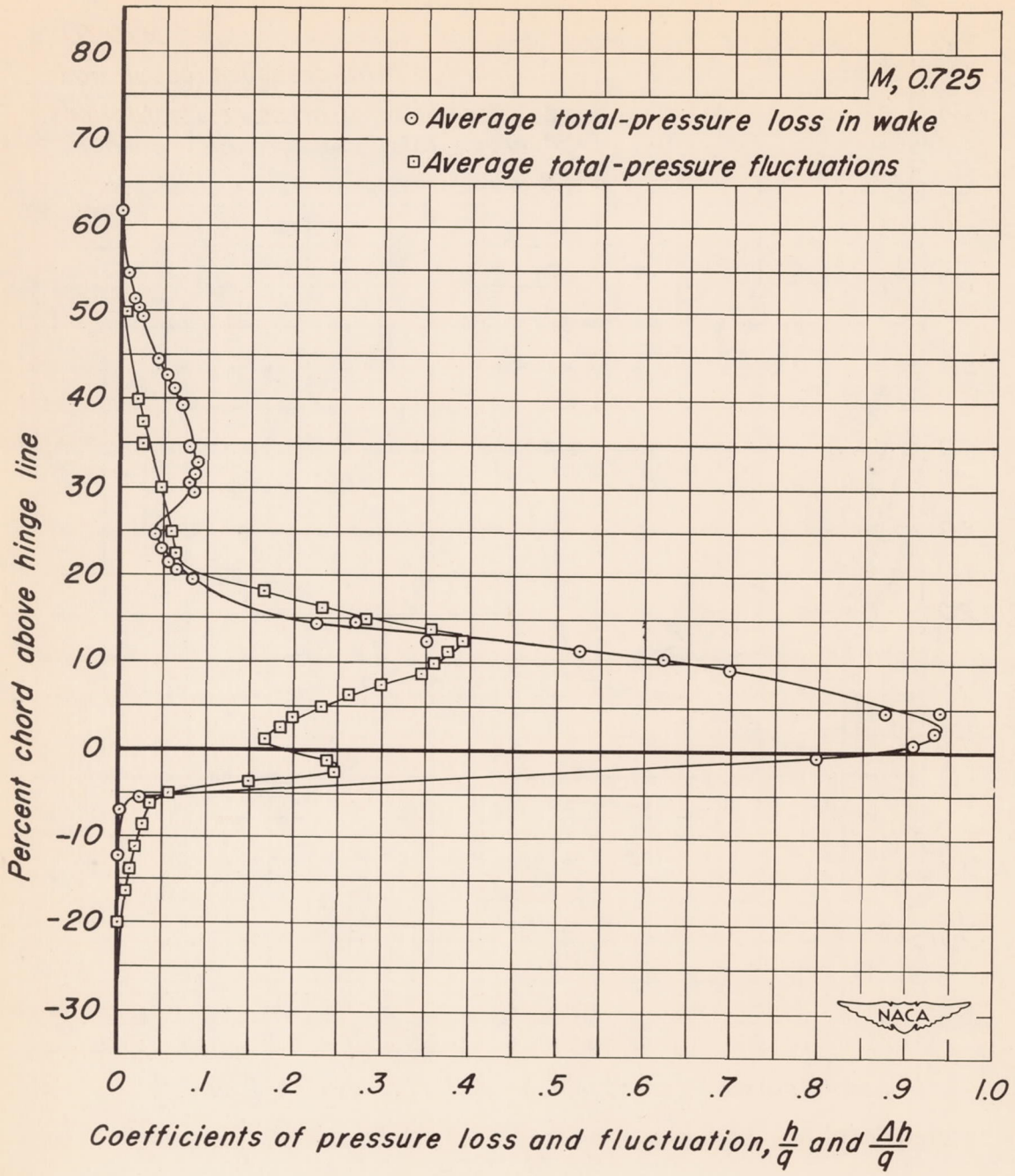

(c) M, 0.725

Figure 17.—Continued.

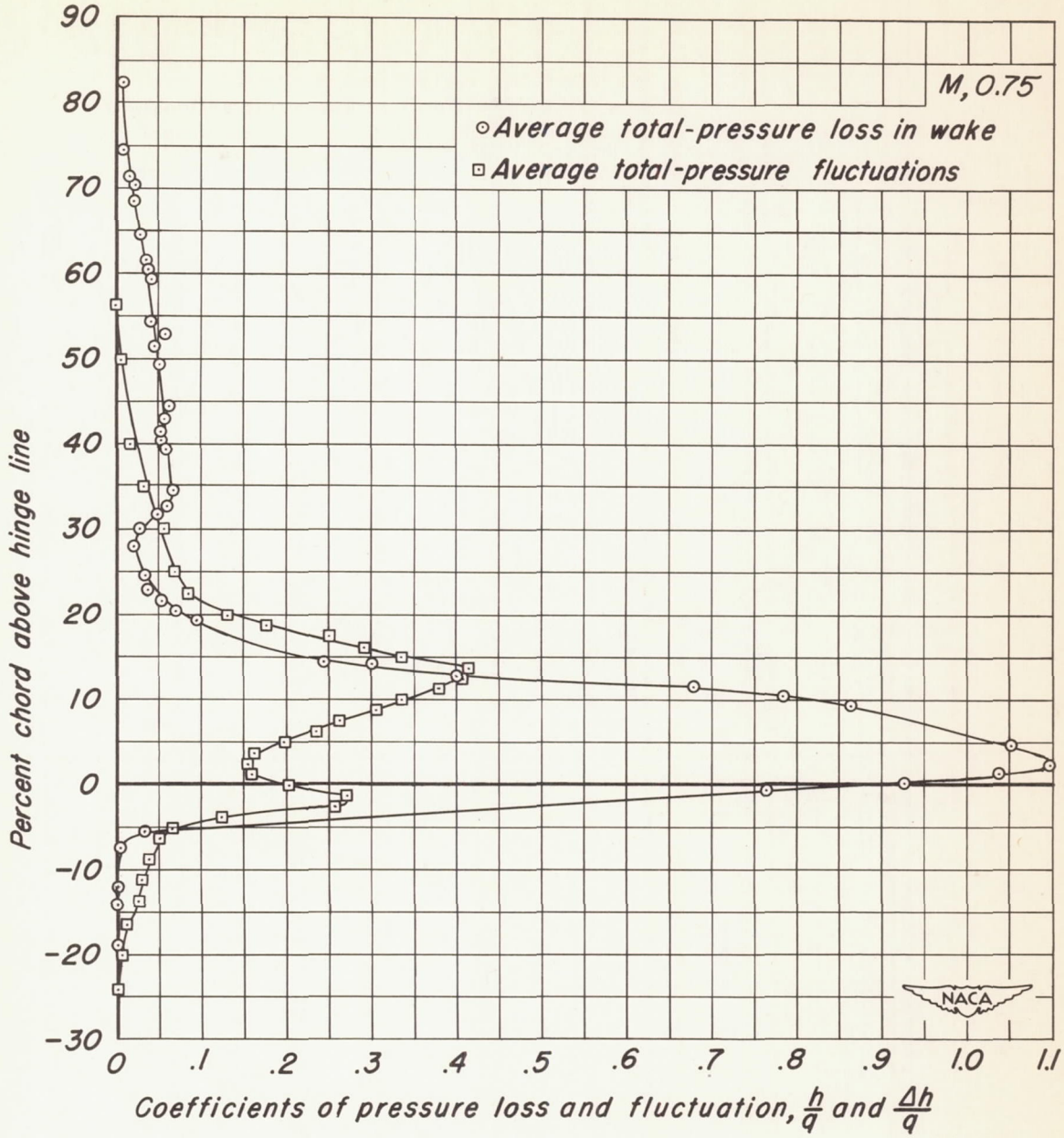

(d) M, 0.75

Figure 17. – Concluded.

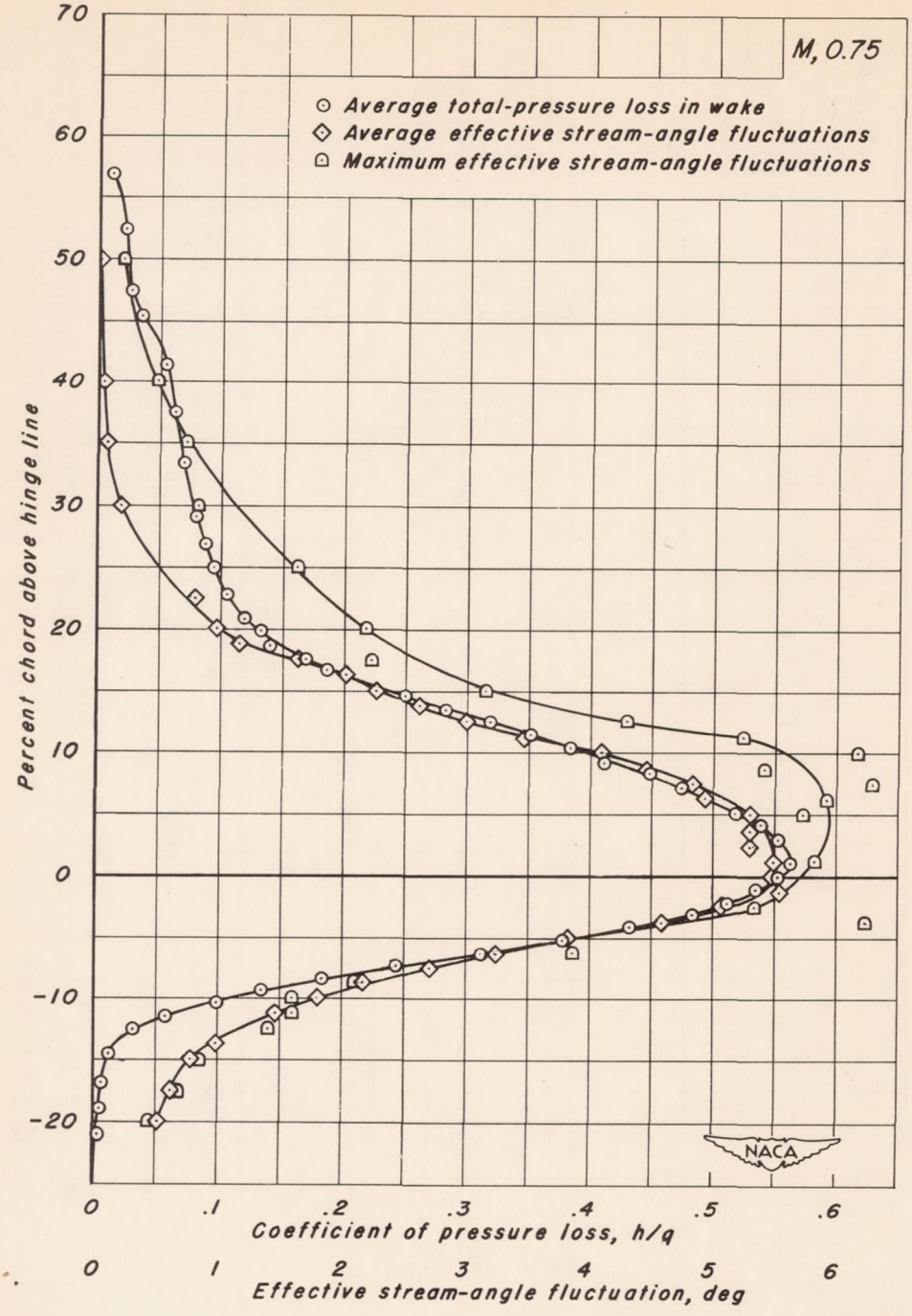

Figure 18.–Wake characteristics at 70-percent-chord aft of the NACA 23013 airfoil. α, +5°; M, 0.75.

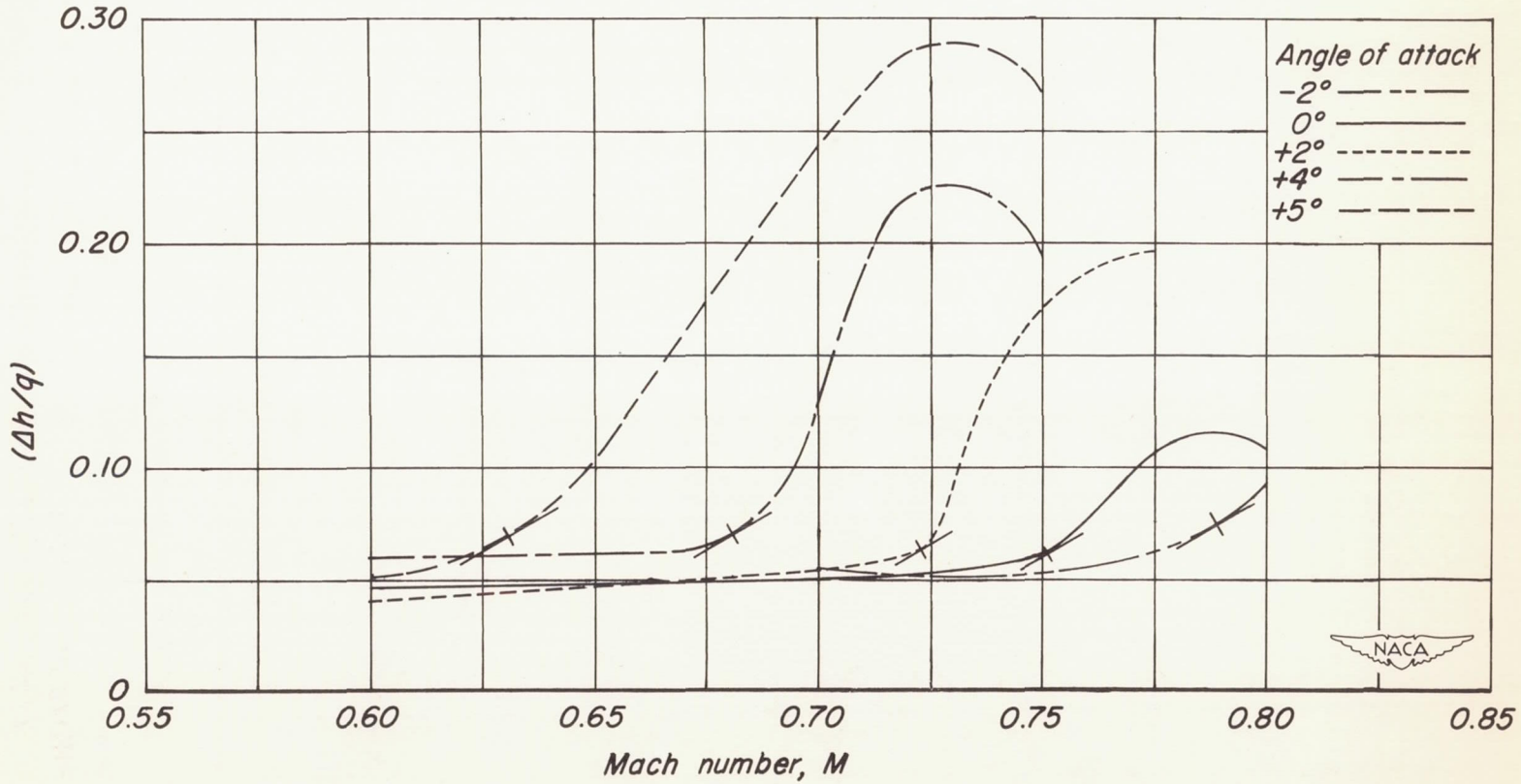

Figure 19.—Plot of the largest amplitude of the average pressure fluctuation 70-percent chord aft of the NACA 23013 airfoil.

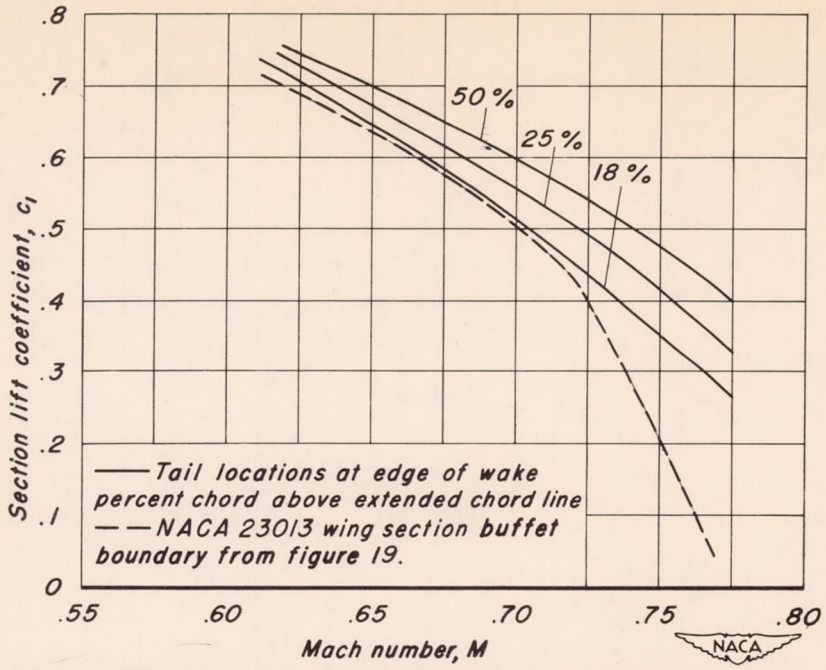

Figure 20.—Wing buffet boundary and horizontal tail location at edge of wake determined from wind-tunnel data.

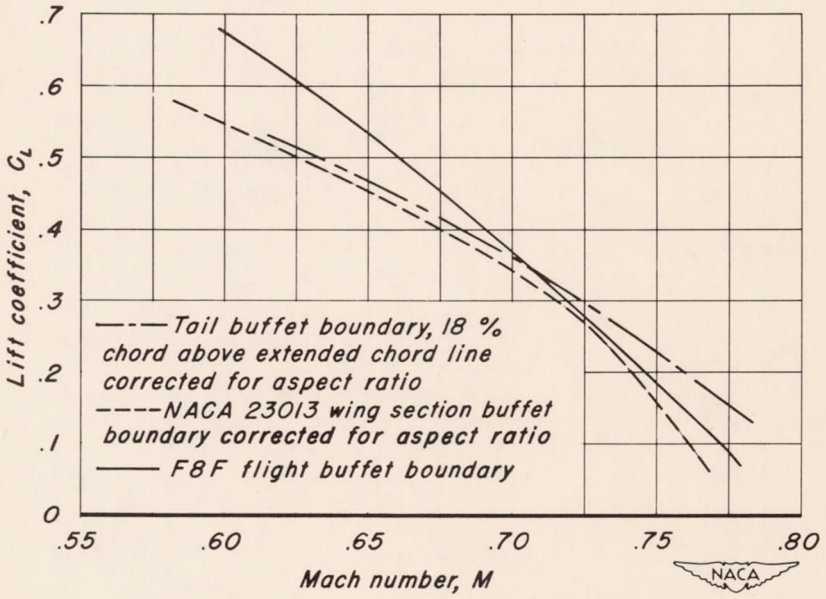

Figure 21.—Comparison of NACA 23013 wing section buffet boundary from wind-tunnel data with airplane buffet boundary determined in flight research.

T-Indicates top surface of airfoil.
B-Indicates bottom surface of airfoil.
Number preceding letter indicates percent chord.

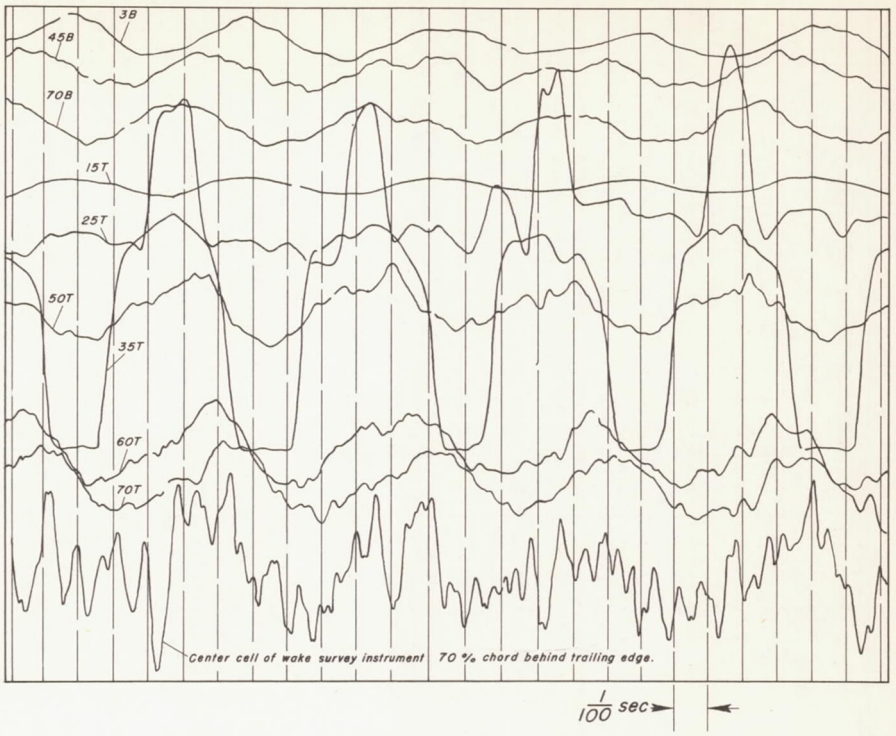

(a) NACA 23013 airfoil. α, 4°; M, 0.725

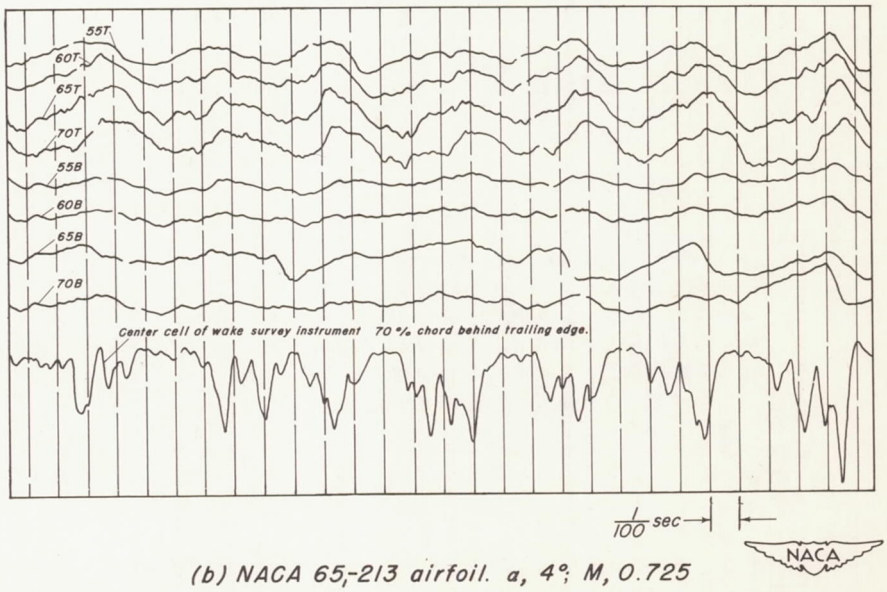

(b) NACA 65$_1$-213 airfoil. α, 4°; M, 0.725

Figure 22.—Illustrations of wake pressure fluctuations at same principal frequency as pressure fluctuations on wing due to shock-wave motion.